EUROPEAN ORGANIZATION FOR NUCLEAR RESEARCH

arXiv:1502.00230v2 [nucl-ex] 29 Jul 2015

Forward-backward multiplicity correlations
in pp collisions at $\sqrt{s} = 0.9$, 2.76 and 7 TeV

ALICE Collaboration[*]

Abstract

The strength of forward-backward (FB) multiplicity correlations is measured by the ALICE detector in proton-proton (pp) collisions at $\sqrt{s} = 0.9$, 2.76 and 7 TeV. The measurement is performed in the central pseudorapidity region ($|\eta| < 0.8$) for the transverse momentum $p_{\mathrm{T}} > 0.3\,\mathrm{GeV}/c$. Two separate pseudorapidity windows of width ($\delta\eta$) ranging from 0.2 to 0.8 are chosen symmetrically around $\eta = 0$. The multiplicity correlation strength (b_{corr}) is studied as a function of the pseudorapidity gap (η_{gap}) between the two windows as well as the width of these windows. The correlation strength is found to decrease with increasing η_{gap} and shows a non-linear increase with $\delta\eta$. A sizable increase of the correlation strength with the collision energy, which cannot be explained exclusively by the increase of the mean multiplicity inside the windows, is observed. The correlation coefficient is also measured for multiplicities in different configurations of two azimuthal sectors selected within the symmetric FB η-windows. Two different contributions, the short-range (SR) and the long-range (LR), are observed. The energy dependence of b_{corr} is found to be weak for the SR component while it is strong for the LR component. Moreover, the correlation coefficient is studied for particles belonging to various transverse momentum intervals chosen to have the same mean multiplicity. Both SR and LR contributions to b_{corr} are found to increase with p_{T} in this case. Results are compared to PYTHIA and PHOJET event generators and to a string-based phenomenological model. The observed dependencies of b_{corr} add new constraints on phenomenological models.

[*]See Appendix B for the list of collaboration members

1 Introduction

We report a detailed study of correlations between multiplicities in pp collisions at 0.9, 2.76 and 7 TeV. The correlations are obtained from event-by-event multiplicity measurements in pseudorapidity (η) and azimuth (φ) separated intervals. The intervals are selected one in the forward and another in the backward hemispheres in the center-of-mass system, therefore the correlations are referred to as forward-backward (FB) correlations.

The FB correlation strength is characterized by the correlation coefficient, b_{corr}, which is obtained from a linear regression analysis of the average multiplicity measured in the backward rapidity hemisphere ($\langle n_{\mathrm{B}} \rangle_{n_{\mathrm{F}}}$) as a function of the event multiplicity in the forward hemisphere (n_{F}):

$$\langle n_{\mathrm{B}} \rangle_{n_{\mathrm{F}}} = a + b_{\mathrm{corr}} \cdot n_{\mathrm{F}} \ . \tag{1}$$

This linear relation (1) has been observed experimentally [1–4] and is discussed in [5–7]. Under the assumption of linear correlation between n_{F} and n_{B}, the Pearson correlation coefficient

$$b_{\mathrm{corr}} = \frac{\langle n_{\mathrm{B}} n_{\mathrm{F}} \rangle - \langle n_{\mathrm{B}} \rangle \langle n_{\mathrm{F}} \rangle}{\langle n_{\mathrm{F}}^2 \rangle - \langle n_{\mathrm{F}} \rangle^2} \tag{2}$$

can be used for the experimental determination of b_{corr} [2]. Since the parameter a is given by $a = \langle n_{\mathrm{B}} \rangle - b_{\mathrm{corr}} \langle n_{\mathrm{F}} \rangle$, it adds no additional information and usually is not considered [5–7].

Heretofore, FB multiplicity correlations were studied experimentally in a large number of collision systems including e^+e^-, μ^+p, pp, p$\overline{\mathrm{p}}$ and A–A interactions [3, 4, 8–13]. No FB multiplicity correlations were observed in e^+e^- annihilation at $\sqrt{s} = 29$ GeV. This was interpreted as the consequence of independent fragmentation of the forward and backward jets produced in this process [14]. In contrast, in pp collisions at the ISR [13] at $\sqrt{s} = 52.6$ GeV [4] and in p$\overline{\mathrm{p}}$ interactions at the Sp$\overline{\mathrm{p}}$S collider [15] sizeable positive FB multiplicity correlations have been observed. Their strength was found to increase strongly with collision energy [3], which was confirmed later at much higher energies ($\sqrt{s} \gtrsim 1$ TeV) in p$\overline{\mathrm{p}}$ collisions by the E735 collaboration at the Tevatron [12] and in pp collisions by the ATLAS experiment at the LHC ($\sqrt{s} = 0.9$ and 7 TeV) [16]. One of the observations reported by ATLAS is the decrease of b_{corr} with the increase of the minimum transverse momentum of charged particles.

The STAR collaboration at RHIC analysed the FB multiplicity correlations in pp and Au–Au collisions at $\sqrt{s_{NN}} = 200$ GeV [17]. Strong correlation was observed in case of Au–Au collisions, while in pp collisions b_{corr} was found to be rather small ($\sim$0.1). In the present paper we relate this to the use of smaller pseudorapidity windows as compared to previous pp and p$\overline{\mathrm{p}}$ measurements.

Forward-backward multiplicity correlations in high energy pp and A–A collisions also raise a considerable theoretical interest. First attempts to explain this phenomenon [7, 18–20] were made in the framework of the Dual Parton Model (DPM) [2] and the Quark Gluon String Model (QGSM) [21, 22]. They provide a quantitative description of multiparticle production in soft processes. In improved versions of the models, collectivity effects arising due to the interactions between strings, which are particularly important in the case of A–A interactions, were taken into account [23–26]. These effects are based on the String Fusion Model (SFM) proposed in [27, 28]. It was shown that these string interactions lead to a considerable modification of the FB correlation strength, along with the reduction of multiplicities, the increase of mean particle p_{T}, and the enhancement of heavy flavour production in central A–A collisions [23, 29, 30].

FB correlations are usually divided into short and long-range components [2, 7]. In phenomenological models, short-range correlations (SRC) are assumed to be localized over a small range of η-differences, up to one unit. They are induced by various short-range effects from single source fragmentation, including particles produced from decays of clusters or resonances, jet and mini-jet induced correlations.

Long-range correlations (LRC) extend over a wider range in η. They originate from fluctuations in the number and properties of particle emitting sources (clusters, cut pomerons, strings, mini-jets etc.) [2, 7, 19, 23–26].

The SFM predicts that the variance of the number of particle-emitting sources (strings) should be damped by their fusion, implying a reduction of multiplicity long-range correlations [23, 25, 26]. Contrary to this prediction, long-range correlations arising in the Color Glass Condensate model (CGC) [31] have been shown to increase with the centrality of the collision [32]. Therefore, the investigation of correlations between various observables, measured in two different, sufficiently separated η-intervals, is considered to be a powerful tool for the exploration of the initial conditions of hadronic interactions [33]. In the case of A–A collisions, these correlations induced across a wide range in η are expected to reflect the earliest stages of the collisions, almost free from final state effects [32, 34]. The reference for the analysis of A–A collision dynamics can be obtained in pp collisions by studying the dependence of FB correlations on collision energy, particle pseudorapidity, azimuth and transverse momenta.

This paper is organized as follows: Section 2 provides experimental details, including the description of the procedures used for the event and track selection, the efficiency corrections and systematic uncertainties estimates. Sections 3 and 4 discuss the results on FB multiplicity correlation measurements in η in pp collisions at $\sqrt{s} = 0.9$, 2.76 and 7 TeV and in η-ϕ windows at $\sqrt{s} = 0.9$ and 7 TeV. In Section 3, we present dependences of the correlation coefficient on the gap between windows, their widths and the collision energy. In Section 4, multiplicity correlations in windows separated in pseudorapidity and azimuth are studied, and the comparison with Monte Carlo generators PYTHIA6 and PHOJET is discussed. Results on multiplicity correlations in different p_T ranges in pp collisions at $\sqrt{s} = 7$ TeV are presented in Section 5.

2 Data Analysis

2.1 Experimental setup, event and track selection

The data presented in this paper were recorded with the ALICE detector [35] in pp collisions at $\sqrt{s} = 0.9$, 2.76 and 7 TeV. Charged primary particles are reconstructed with the central barrel detectors combining information from the Inner Tracking System (ITS) and the Time Projection Chamber (TPC). Both detectors are located inside the 0.5 T solenoidal field.

The ITS is composed of 3 different types of coordinate-sensitive Si-detectors. It consists of 2 silicon pixel innermost layers (SPD), 2 silicon drift (SDD) and 2 silicon strip (SSD) outer detector layers. The design allows for two-particle separation in events with multiplicity up to 100 charged particles per cm^2. The SPD detector covers the pseudorapidity ranges $|\eta| < 2$ for inner and $|\eta| < 1.4$ for outer layers, acceptances of SDD and SSD are $|\eta| < 0.9$ and $|\eta| < 1$, respectively. All ITS elements have a radiation length of about 1.1% X_0 per layer. The ITS provides reliable charged particle tracking down to transverse momenta of 0.1 GeV/c, ideal for the study of low-p_T (soft) phenomena.

The ALICE TPC is the main tracking detector of the central rapidity region. The TPC, together with the ITS, provides charged particle momentum measurement, particle identification and vertex determination with good momentum and dE/dx resolution as well as two-track separation of identified hadrons and leptons in the p_T region below 10 GeV/c. The TPC has an acceptance of $|\eta| < 0.9$ for tracks which reach the outer radius of the TPC and up to $|\eta| < 1.5$ for tracks that exit through the endcap of the TPC.

For the present analysis, minimum bias pp events are used. The minimum-bias trigger required a hit in one of the forward scintillator counters (VZERO) or in one of the two SPD layers. The VZERO timing signal was used to reject beam-gas and beam-halo collisions. The primary vertex was reconstructed using the combined track information from the TPC and ITS, and only events with primary vertices lying within ±10 cm from the centre of the apparatus are selected. In this way a uniform acceptance in
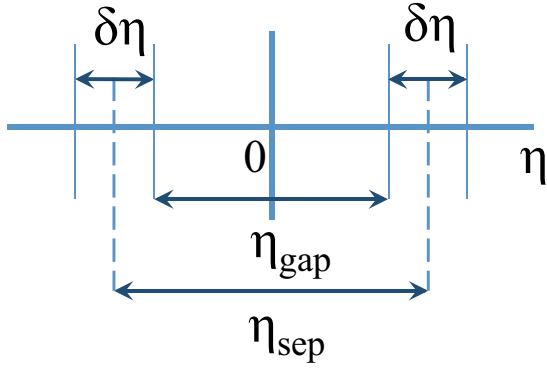
Fig. 1: Illustration of the variables $\delta\eta$, η_{gap} and η_{sep} used in the present analysis.

Fig. 2: Illustration of sets of η-windows with different widths $\delta\eta$ and separation gaps η_{gap}.
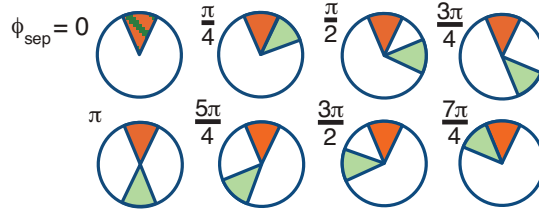

Fig. 3: Illustration of 8 configurations of azimuthal sectors. Forward and backward pseudorapidity windows of the width $\delta\eta = 0.2$ are additionally split into 8 azimuthal sectors with the width $\delta\varphi = \pi/4$. The red sectors correspond to the first window of the FB pair, the green sectors to the second one. The variable φ_{sep} is the separation in azimuthal angle between centres of the sectors.

the central pseudorapidity region $|\eta| < 0.8$ is ensured. The data samples for $\sqrt{s} = 0.9$, 2.76 and 7 TeV comprise 2×10^6, 10×10^6, and 6.5×10^6 events, respectively. Only runs with low probability to produce several separate events per one bunch crossing (so-called pile-up events) were used in this analysis.

To obtain high tracking efficiency and to reduce efficiency losses due to detector boundaries, tracks are selected with $p_{\text{T}} > 0.3\,\text{GeV}/c$ in the pseudorapidity range $|\eta| < 0.8$. Employing a Kalman filter technique, tracks are reconstructed using space-time points measured by the TPC. Tracks with at least 70 space-points associated and track fitting χ^2/n_{dof} less than 2 are accepted. Additionally, at least two hits in the ITS must be associated with the track. Tracks are also rejected if their distance of closest approach (DCA) to the reconstructed event vertex is larger than 0.3 cm in either the transverse or the longitudinal plane. For the chosen selection criteria, the tracking efficiency for charged particles with $p_{\text{T}} > 0.3\,\text{GeV}/c$ is about 80%.

2.2 Definition of counting windows

Two intervals separated symmetrically around $\eta = 0$ with variable width $\delta\eta$ ranging from 0.2 to 0.8 are defined as "forward" (F, $\eta > 0$) and "backward" (B, $\eta < 0$). Correlations between multiplicities of charged particles (n) are studied as a function of the gap between the windows (denoted as η_{gap}). Another convenient variable is η_{sep} which is the separation in pseudorapidity between centres of the windows. These variables are illustrated in Fig. 1, and all configurations of window pairs chosen for the analysis are drawn in Fig. 2.

The analysis is extended to correlations between separated regions in the η-φ plane (sectors). The φ-angle space is split into 8 sectors with the width $\delta\varphi = \pi/4$ as shown in Fig. 3. This selection is motivated by a compromise between granularity and statistical uncertainty. The definitions and equations, described in Section 1, remain the same for the η-φ windows. The acceptance of the windows is determined by
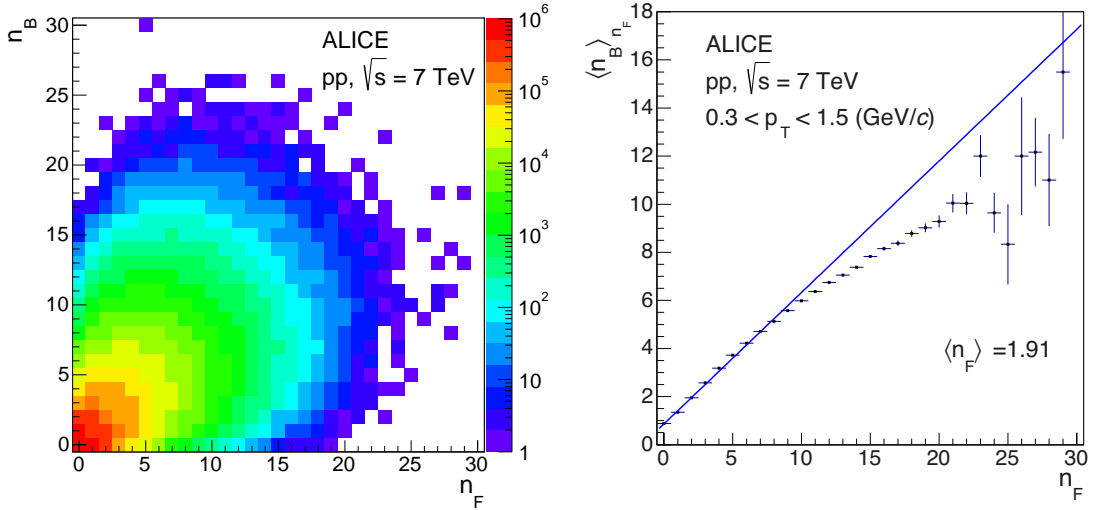
Fig. 4: Illustrative example of forward versus backward raw multiplicity distribution for windows with $\delta\eta = 0.6$ and $\eta_{\text{gap}} = 0.4$ at $\sqrt{s} = 7$ TeV (left) and corresponding correlation function (right). The correlation strength b_{corr} is obtained from a linear fit according to Eq. 1. Since most of the statistics is at low multiplicities, the fit is mainly determined by the first points.

their widths $\delta\eta$ and $\delta\varphi$ as the ALICE acceptance is approximately uniform in the selected ranges of η and φ.

2.3 Experimental procedures of the FB correlation coefficient measurement

The present paper focuses on the study of FB correlation phenomena related to soft particle production. Therefore we restrict p_T in $0.3 < p_T < 1.5$ GeV/c, except for the study of the p_T dependence presented in Section 5, where the p_T range is $0.3 < p_T < 6$ GeV/c.

The correlation coefficients, b_{corr}, for each window pair can be calculated using two methods [1–4]. In the first method values of $\langle n_B n_F \rangle$, $\langle n_B \rangle$, $\langle n_F \rangle$ and $\langle n_F^2 \rangle$ are accumulated event-by-event and then b_{corr} is determined using Eq. 2. In the second method, b_{corr} is calculated using linear regression. The 2-dimensional distributions (n_B, n_F) are obtained integrating over all selected events, then the average backward multiplicity is calculated for each fixed value of the forward multiplicity, and b_{corr} is obtained from a linear fit to the correlation function (see illustration in Fig. 4). Deviations from linear behavior may provide additional information, however, a detailed study of non-linearity in the correlation function is beyond the scope of this paper.

It has been shown that the results obtained with the two methods agree within statistical uncertainty. In this work, results using the first method are presented.

2.4 Corrections and systematic uncertainties

Acceptance and tracking efficiency corrections are extracted from Monte Carlo simulations using PYTHIA6 [36] (Perugia 0 tune) and PHOJET [37, 38] as particle generators followed by a full detector response simulation based on GEANT3 [39]. Corrections are done to primary charged particle correlations and multiplicities. Correction factors obtained with these two generators are found to agree within 1% and the difference is neglected. Three independent correction procedures are investigated.

In the first procedure, the correction factors for b_{corr} are obtained as the ratio of b_{corr} obtained at generator level (true value) to b_{corr} after detector response simulation (measured value). In the second procedure the correction factors are obtained for $\langle n_B n_F \rangle$, $\langle n_B \rangle$, $\langle n_F \rangle$ and $\langle n_F^2 \rangle$ separately and b_{corr} is obtained from the corrected moments. The third procedure takes into account approximately linear dependence of b_{corr}

Error source	0.9 TeV	2.76 TeV	7 TeV
Number of TPC space-points	0.5–3.0	0–0.1	0.2–0.7
Number of ITS space-points	0.6–1.9	–	0.2–1.4
DCA	3.0–4.0	1.0–1.8	0.1–1.0
Vertex position along the beam line	0.2–1.1	0–1.0	0–0.7
b_{corr} correction procedure	2.5–4.0	2.2–4.2	1.6–2.8
Event pile-up	<1	<1	<1
Total (%)	3.4–4.5	2.8–4.2	2.0–3.0

Table 1: Sources of systematic errors of b_{corr} measurements in η-windows of width $\delta\eta = 0.2$, and their contributions (in %). The minimal and maximal estimated values are indicated for each given source.

on $\langle n_{\text{F}} \rangle$ when $\langle n_{\text{F}} \rangle$ varies with cuts, and each corrected value of b_{corr} is found by extrapolation to the corrected value of $\langle n_{\text{F}} \rangle$.

It was found that results of all three procedures agree within 1.6-4.2% (see Table 1), thus proving the robustness of b_{corr} determination. The second procedure was chosen as the most direct and commonly used to produce the final corrected value of b_{corr}. Correction factors increase the values of b_{corr}, obtained for standard cuts, by 6-10 % for analysis in η-windows and 9-18 % for analysis in η-ϕ windows and in p_{T} intervals. By varying the selection cuts (vertex- , DCA- and track selection cuts), correction procedures, and by comparison of the high and low pile-up runs, the systematic uncertainties on b_{corr} have been estimated. Adding all contributions in quadrature, the total systematic uncertainties are below 4.5% (4.2%, 3%) at $\sqrt{s} = 0.9$ (2.76, 7) TeV for the b_{corr} analysis in η-separated windows, and 6% for analysis in η-ϕ separated windows at $\sqrt{s} = 0.9$ and 7 TeV. For the b_{corr} analysis in p_{T} intervals for 7 TeV, the systematic uncertainties are less than 8%. Statistical errors are small and within the symbol sizes for data points in the figures. A summary of the contributions of systematic uncertainties for b_{corr} in η-separated windows with the width $\delta\eta = 0.2$ is presented in Table 1.

3 Multiplicity correlations in windows separated in pseudorapidity

3.1 Dependence on the gap between windows

Fig. 5 shows the FB multiplicity correlation coefficient b_{corr} as a function of η_{gap} and for different widths of the η windows ($\delta\eta$) in pp collisions at the three collision energies. For each $\sqrt{s}$, b_{corr} is found to decrease slowly with increasing η_{gap}, while maintaining a substantial pedestal value throughout the full

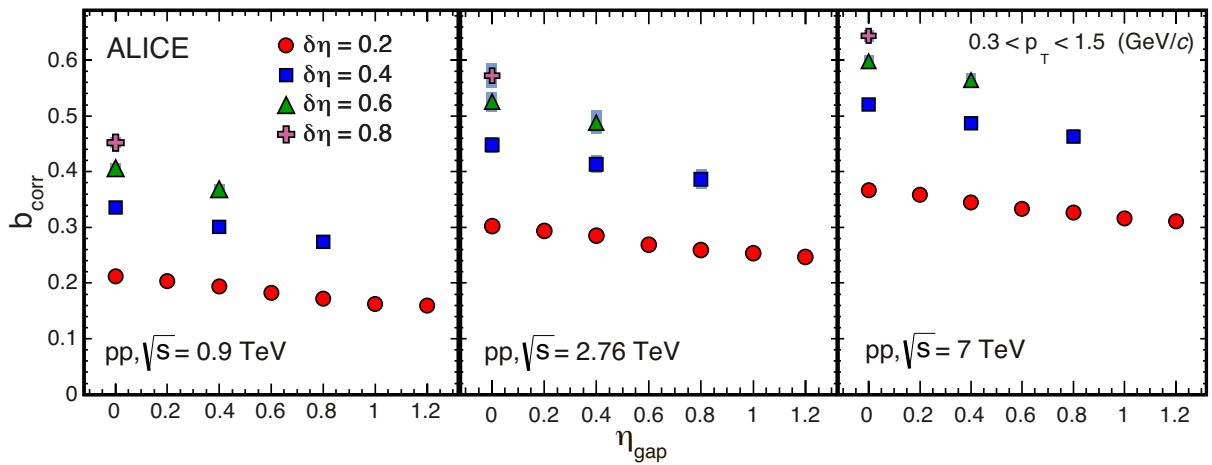**Fig. 5:** Forward-backward correlation strength b_{corr} as function of η_{gap} and for different windows widths $\delta\eta$=0.2, 0.4, 0.6 and 0.8 in pp collisions at $\sqrt{s} = 0.9$, 2.76 and 7 TeV.
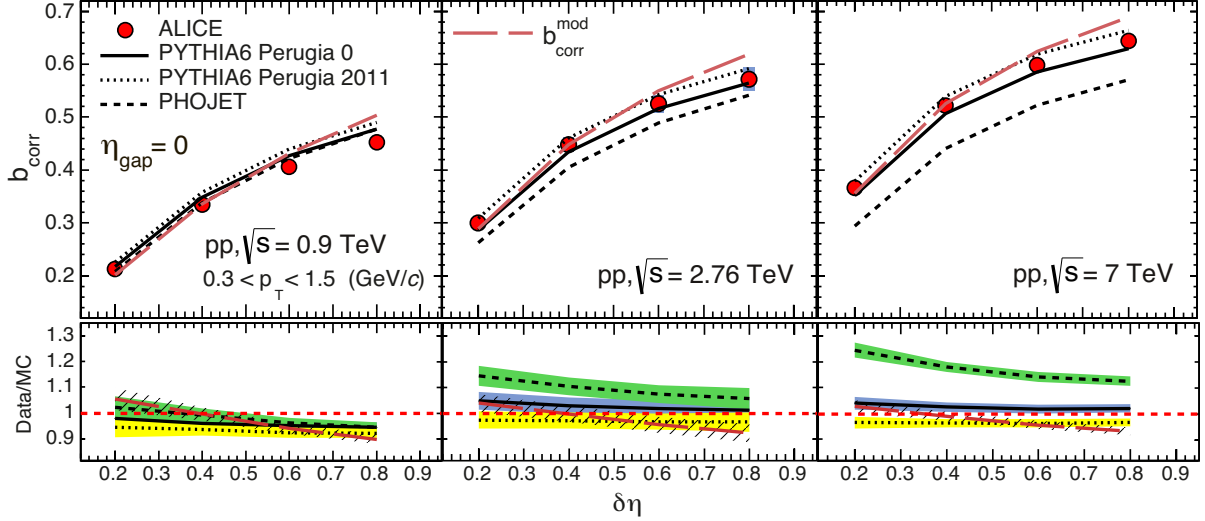
Fig. 6: Correlation strength b_{corr} as a function of $\delta\eta$ for $\eta_{gap} = 0$ in pp collisions for $\sqrt{s} = 0.9$, 2.76 and 7 TeV. The MC results from PYTHIA6 Perugia 0 (solid line), Perugia 2011 (dotted line) and PHOJET (dashed line), calculated at generator level, are shown for comparison. The bottom panels show the ratio of b_{corr} between data and MC. The red dashed curves correspond to the model of independent particle emission from a fluctuating source (see text).

η_{gap} range.

3.2 Dependence on the width of windows

The $\delta\eta$-dependence for adjacent ($\eta_{gap} = 0$), symmetrical windows with respect to $\eta = 0$ is shown in Fig. 6. For all collision energies, the correlation coefficient increases non-linearly with $\delta\eta$. This trend is quite well described by PYTHIA6 and PHOJET, although the agreement worsens with increasing $\sqrt{s}$. This $\delta\eta$-dependence can be understood, along with other approaches [7, 25, 40], in a simple model with event-by-event multiplicity fluctuations and random distribution of produced particles in pseudorapidity. In this model, the multiplicity in an η interval containing the fraction p of the mean multiplicity $\langle N \rangle$ in the full η-acceptance is binomially distributed and its mean square is given by

$$\langle n_F^2 \rangle = \langle n_B^2 \rangle = p(1-p)\langle N \rangle + p^2 \langle N^2 \rangle \,, \tag{3}$$

where N is the charged particle multiplicity measured in the pseudorapidity interval Y and

$$p = \frac{\langle n_F \rangle}{\langle N \rangle} = \frac{\langle n_B \rangle}{\langle N \rangle} = \frac{\delta\eta}{Y} \,. \tag{4}$$

One can connect the multiplicity fluctuations in the full η-acceptance considered in this analysis ($Y = 1.6$) with the correlation strength b_{corr} (see Appendix A):

$$b_{corr}^{mod} = \frac{\alpha\delta\eta/Y}{1 + \alpha\delta\eta/Y} \,, \tag{5}$$

where

$$\alpha = \frac{\sigma_N^2}{\langle N \rangle} - 1 \,. \tag{6}$$

Note that using Eq. 3 and Eq. 4 one can write the Eq. 5 also in the following form:

$$b_{corr}^{mod} = 1 - \frac{\langle n_F \rangle}{\sigma_{n_F}^2} \,. \tag{7}$$

$\sqrt{s}$ (TeV)	window width $\delta\eta$	$\langle n_F \rangle$	b_{corr} (η_{gap}=0)	b_{corr} (max. η_{gap})
0.9	0.54	1.17	0.39 ± 0.01	0.35 ± 0.01
2.76	0.4	1.17	0.44 ± 0.02	0.38 ± 0.02
7	0.33	1.17	0.48 ± 0.01	0.43 ± 0.01

Table 2: Correlation strength b_{corr} in pp collisions at $\sqrt{s} = 0.9$, 2.76 and 7 TeV in windows with equal mean multiplicity $\langle n_F \rangle$ and the corresponding values of $\delta\eta$. Values are shown for adjacent windows (η_{gap}=0) and for windows with maximal η_{gap} within $|\eta| < 0.8$. The uncertainty on $\langle n_F \rangle$ is about 0.001.

From the measured ratio of the multiplicity variance $\sigma_N^2 \equiv \langle N^2 \rangle - \langle N \rangle^2$ in $Y = 1.6$ to the mean value $\langle N \rangle$ we obtain the value of α at $\sqrt{s} = 0.9$, 2.76 and 7 TeV to be 2.03, 3.25 and 4.42, respectively, with a systematic uncertainty of about 5%. The $b_{\mathrm{corr}}^{\mathrm{mod}}(\delta\eta)$-dependences calculated by Eq. 5 are shown in Fig. 6 as red dashed lines. At $\eta_{\mathrm{gap}} = 0$ the $b_{\mathrm{corr}}(\delta\eta)$ dependence is well described by this simple model. However, this model is not able to describe the dependence of b_{corr} on η_{gap} in Fig. 5 because it does not take into account the SRC contribution mentioned above.

3.3 Dependence on the collision energy

Figure 5 shows that the pedestal value of b_{corr} increases with $\sqrt{s}$, while the slope of the $b_{\mathrm{corr}}(\eta_{\mathrm{gap}})$ dependence stays approximately constant. This indicates that the contribution of the short-range correlations has a very weak $\sqrt{s}$-dependence, while the long-range multiplicity correlations play a dominant role in pp collisions and their strength increases significantly with $\sqrt{s}$. Note that this increase cannot be explained by the increase of the mean multiplicity alone. If, at different energies, we choose window sizes such that the mean multiplicity stays constant the increase is still observed (see Table 2).

In the framework of the simple model described by Eq. 5 and 6 the increase of the correlation coefficient corresponds to the increase of the event-by-event multiplicity fluctuations with $\sqrt{s}$ characterized by the ratio $\sigma_N^2/\langle N \rangle$.

A strong energy dependence and rather large b_{corr} values were previously reported by the UA5 collaboration [3] and recently by the ATLAS Collaboration [16]. However, as we see in Fig. 6, the correlation coefficient depends in a non-linear way on the width of the pseudorapidity window. One has to take this fact into account when comparing the correlation strengths obtained under different experimental conditions. In particular, it explains the small values of b_{corr} observed by the STAR collaboration at RHIC (pp, $\sqrt{s} = 200$ GeV) [17], where narrow FB windows ($\delta\eta = 0.2$) were considered, while in previous pp and p$\bar{\mathrm{p}}$ experiments wider windows of a few units of pseudorapidity were used.

4 Multiplicity correlations in windows separated in pseudorapidity and azimuth

Multiplicity correlations are also studied in different configurations of forward and backward azimuthal sectors. These sectors are chosen in separated forward and backward pseudorapidity windows of width $\delta\eta = 0.2$ and $\delta\varphi = \pi/4$ as shown in Fig. 3, resulting in 5 pairs with different φ-separation.

Figs. 7 and 8 show the azimuthal dependence of b_{corr} as a function of different η_{sep}, for 0.9 and 7 TeV, respectively. Data are compared to PYTHIA6 (tunes Perugia 0 and Perugia 2011), PHOJET and a parametric string model [41].

The string model fitted to our data helps to understand in a simple way the origins of the b_{corr} behaviour. There are two contributions to b_{corr} in this model. The short-range (SR) contribution originating from the correlation between particles produced from the decay of a single string and the long-range (LR) contribution arising from event-by-event fluctuations of the number of strings. The energy dependence of the fitted parameters demonstrates that SR parameters stay constant with $\sqrt{s}$ while the normalized variance of the number of strings, the only LR parameter of the model, increases by a factor of three.
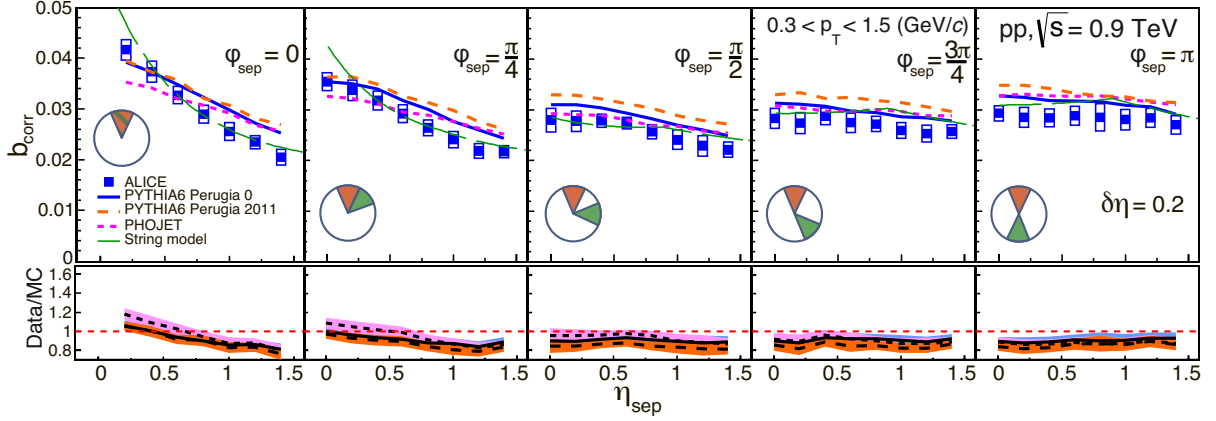
8

Fig. 7: Correlation strength b_{corr} for separated η-φ window pairs at $\sqrt{s} = 0.9$ TeV as a function of η separation, with fixed window width $\delta\eta$=0.2 and $\delta\varphi$=π/4. The panels are for different separation distances between the two azimuthal sectors: $\varphi_{sep} = 0$, $\pi/4$, $\pi/2$, $(3/4)\pi$ and π. MC results from PYTHIA6 Perugia 0 (blue lines), Perugia 2011 (orange dashed lines) and PHOJET (pink dashed lines) and string model [41] (thin green lines) are also shown. The bottom panels show the ratio b_{corr} between data and MC results.

Fig. 8: Correlation strength b_{corr} for separated η-φ window pairs at $\sqrt{s} = 7$ TeV as a function of η separation. The legend is the same as for Fig. 7.

The 2-dimensional distribution of b_{corr} as a function of η_{sep} and φ_{sep} is shown in Fig. 9 for $\sqrt{s} = 0.9$ and 7 TeV. The qualitative behaviour of b_{corr} resembles the results obtained for two-particle angular correlations: near-side peak and recoil away-side structure. The connection between the FB correlation and two-particle correlation function is discussed in detail in [7, 41–43].

The shapes of the correlation functions clearly indicate two contributions to the forward-backward multiplicity correlation coefficient. The SR contribution is concentrated within a rather limited region in the η-φ plane within one unit of pseudorapidity and $\pi/2$ in azimuth, while the LR contribution manifests itself as a common pedestal in the whole region of observation.

The strength of multiplicity correlations measured in η and η-φ windows is compared to the results obtained with PYTHIA6 [36] (tunes Perugia 0 and Perugia 2011) and PHOJET [37, 38] Monte Carlo generators (MC). The detailed overview of key features of these generators can be found in [44]. Recent Perugia tunes for PYTHIA6 are described in [45].

In Fig. 10 the comparison of b_{corr} as a function of η_{gap} for $\delta\eta = 0.2$ at $\sqrt{s} = 0.9$, 2.76 and 7 TeV with the results obtained with different MC generators is shown. All models describe the data at $\sqrt{s} = 0.9$ TeV reasonably well, while larger discrepancies are observed at 2.76 and 7 TeV, with PYTHIA giving a
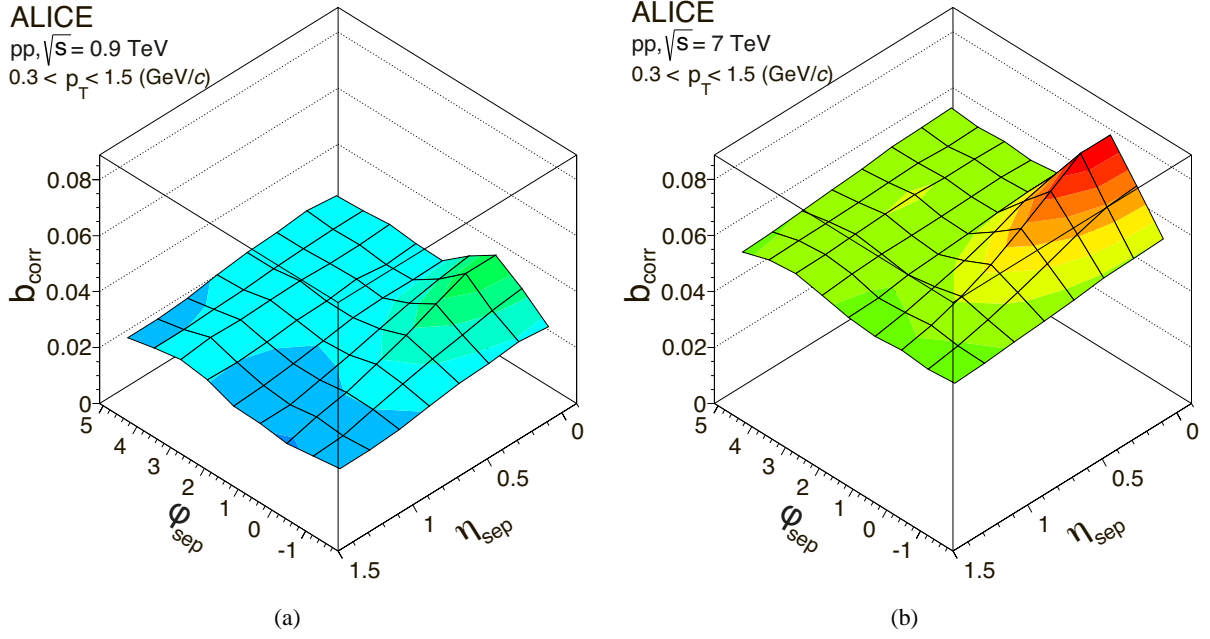
Fig. 9: 2D representation of b_{corr} at (a) $\sqrt{s} = 0.9$ TeV and (b) at $\sqrt{s} = 7$ TeV for separated η-φ window pairs with $\delta\eta$=0.2 and $\delta\varphi$=$\pi/4$. To improve visibility, the point $(\eta_{sep}, \varphi_{sep})$=(0,0) and thus b_{corr}=1 is limited to the level of the maximum value in adjacent bins.

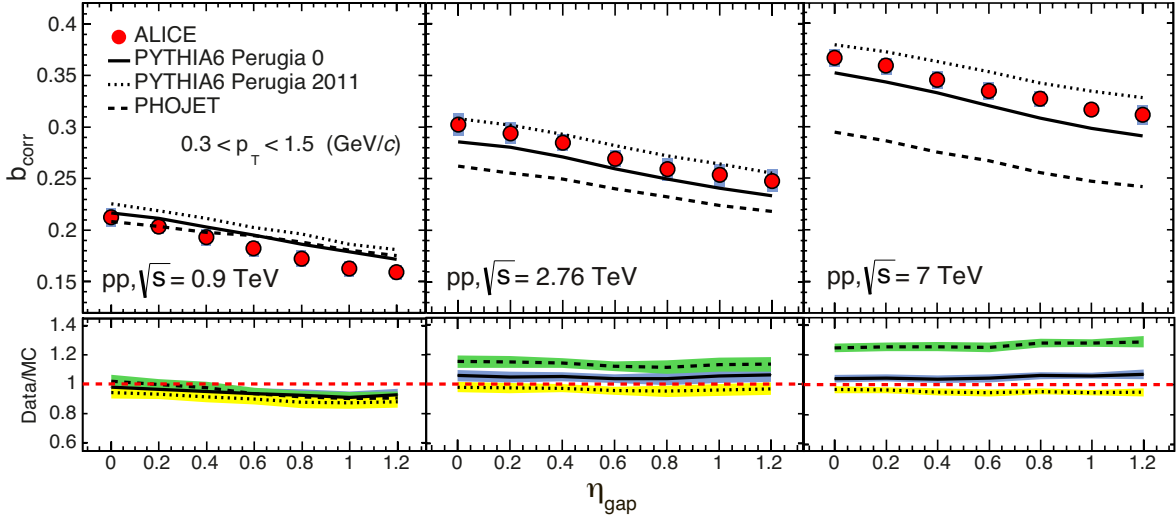**Fig. 10:** Correlation strength b_{corr} as a function of η_{gap} in pp collisions for data taken from Fig. 5 and compared to MC generators PYTHIA Perugia 0 (solid line), Perugia 2011 (dotted line) and PHOJET (dashed line) for $\sqrt{s} = 0.9$, 2.76 and 7 TeV collision energies, windows width $\delta\eta$ is 0.2. The bottom panels show the ratio of the data to MC.

better description of the data than PHOJET. Qualitatively similar conclusions can be drawn from the comparison of the $\delta\eta$-dependence in experimental data and MC as shown in Fig. 6.

Note that PYTHIA also describes the correlations in η-φ windows reasonably well, see Figures 7 and 8, while PHOJET gives a good description only for $\sqrt{s} = 0.9$ TeV and significantly underestimates the data at 7 TeV.

The difference between the experimental data and the results obtained with MC generators is more visible in Fig. 11, which compares the measured ratio of b_{corr} at $\sqrt{s} = 2.76$ and 7 TeV with respect to 0.9 TeV as a function of η_{gap} to MC calculations. The measured ratios show an increasing trend as a function of
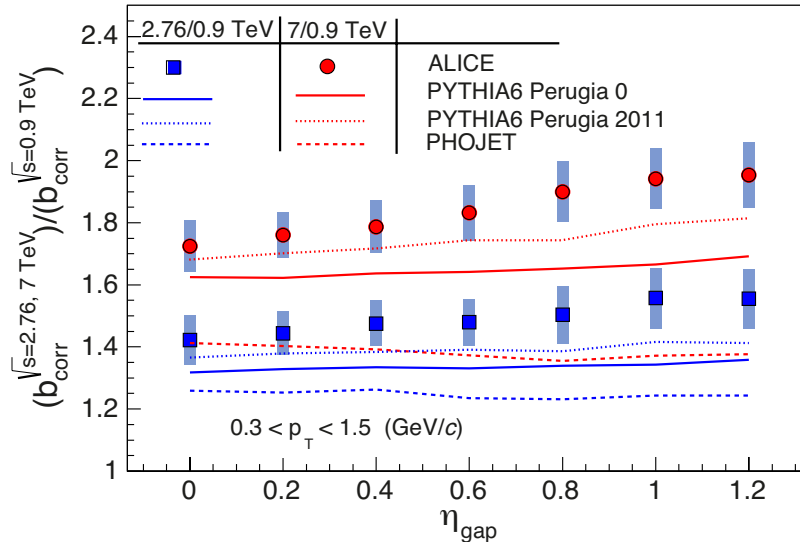
Fig. 11: Ratio of b_{corr} at 2.76 (blue squares) and 7 TeV (red circles) with respect to 0.9 TeV vs. η_{gap}. The calculations from MC generators are also shown: PYTHIA Perugia 0 (solid line), Perugia 2011 (dotted line) and PHOJET (dashed line), for 2.76 TeV (blue lines) and 7 TeV (red lines).

η_{gap}, while PYTHIA and PHOJET underestimate the ratios and exhibit a flatter η_{gap} dependence.

It is important to note that, in the framework of PYTHIA, the observed LR part of b_{corr} (the pedestal in Fig. 9) is dominated by multiple parton-parton interactions (MPI). This supports earlier results [46], in which the FB correlations in pp collisions were studied by MC simulations with recent tunes of the PYTHIA6 at $\sqrt{s} = 0.9$ TeV. Hence, the observed dependence of b_{corr} on collision energy and on different configurations of rapidity and azimuthal windows adds new constraints on phenomenological models for multi-particle production.

5 Dependence of FB multiplicity correlation strength on the choice of p_T intervals

The behaviour of FB multiplicity correlation strength was also studied as a function of p_T of registered particles. These studies were motivated by a recent paper by the ATLAS collaboration [16], which reported a decrease in the multiplicity correlation strength with increasing p_T^{min}. However, as we have observed in Section 3.2, there is a strong non-linear dependence of b_{corr} on the size of pseudorapidity windows and, hence, on the mean multiplicity $\langle n_{ch} \rangle$ in the window (see Eq. 4, 5, and Fig. 6). In order to demonstrate that the strong p_T^{min} dependence is not a trivial multiplicity dependence, in our analysis we use p_T intervals with the same $\langle n_{ch} \rangle$. To this end, the correlation strength b_{corr} is studied for five p_T intervals within $0.3 < p_T < 6$ GeV/c at $\sqrt{s} = 7$ TeV: 0.3–0.4, 0.4–0.52, 0.52–0.7, 0.7–1.03 and 1.03–6.0 (GeV/c). In each p_T interval, the corrected mean multiplicity $\langle n_F \rangle = 0.157$ with a systematic uncertainty about 2%. Correlations are studied in η and η-φ FB-windows configurations. Note that in case of windows chosen symmetrically with respect to $\eta = 0$ the definition of b_{corr} given by (2) coincides with the correlation coefficient ρ_{FB}^n used in the ATLAS analysis.

Fig. 12 shows b_{corr} as a function of p_T^{min} for $\eta_{gap} = 0$ and 1.2. Systematic uncertainties are shown as rectangles, statistical uncertainties are negligible. We find that b_{corr} increases with p_T^{min} for both values of η_{gap}, in contrast to the results reported in [16]. This result can be understood if one takes into account that the multiplicity fluctuations in a given window are closely connected with the two-particle correlation strength [7, 43]. In the simple model with the event-by-event multiplicity fluctuations and random distribution of produced particles in pseudorapidity, discussed in Section 3.2, Eq. 7 allows us to discuss the observed dependence of the correlation coefficient b_{corr} on the p_T-binnings for the case of
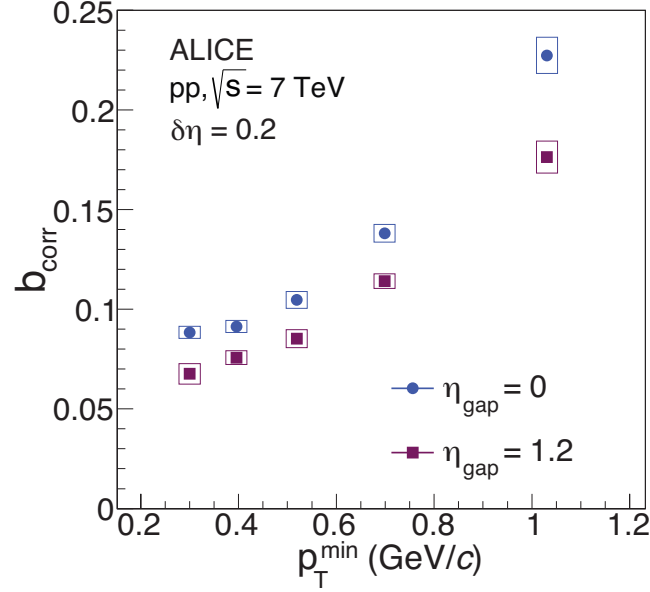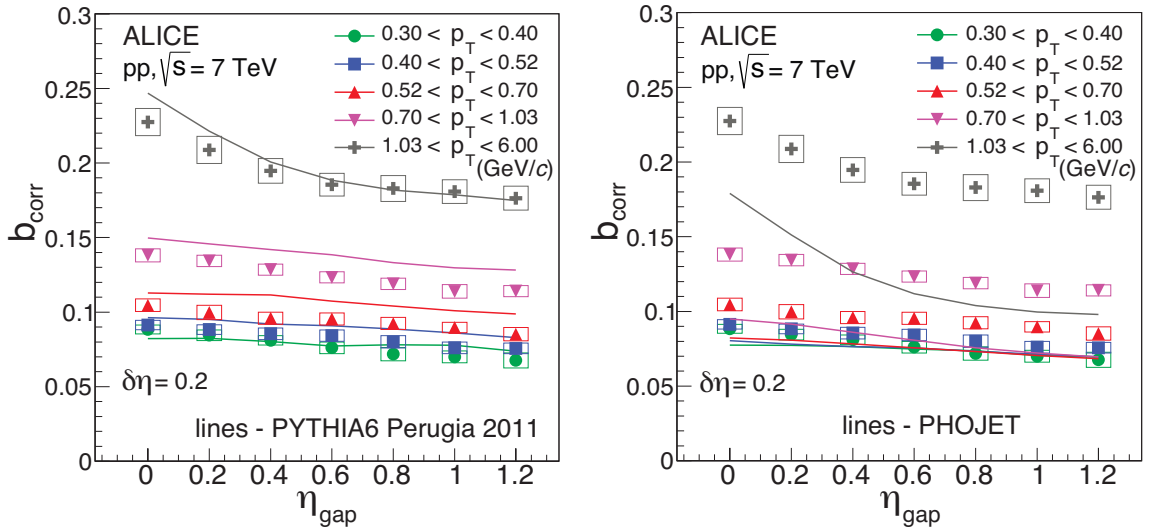
Fig. 12: Correlation strength b_{corr} at $\sqrt{s} = 7$ TeV for separated pseudorapidity window pairs, measured in p_T intervals with same $\langle n_{ch} \rangle$, as a function of p_T^{min} for each interval. Values are shown for η_{gap}=0, 1.2 with $\delta\eta$=0.2.

Fig. 13: Correlation strength b_{corr} at $\sqrt{s} = 7$ TeV for separated pseudorapidity window pairs, measured in p_T intervals with same $\langle n_{ch} \rangle$ as a function of η_{gap}. Windows of width $\delta\eta$=0.2. Left and right panels contain same data points, lines correspond to PYTHIA6 Perugia 2011 (left) and to PHOJET (right).
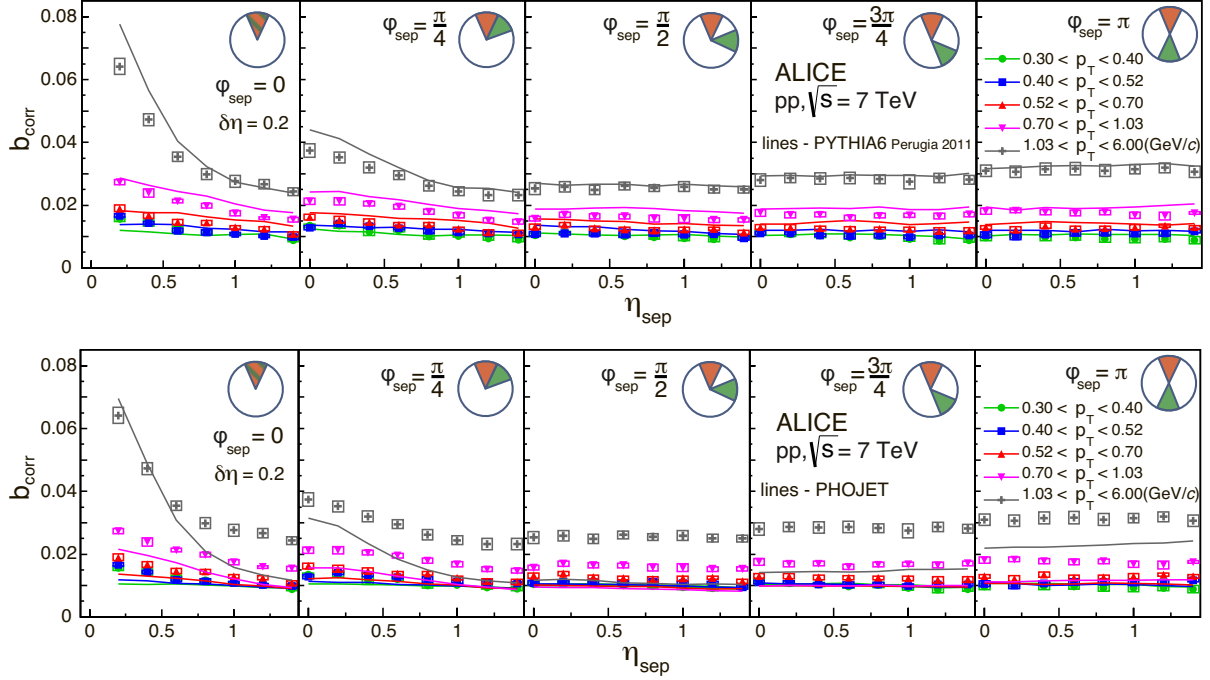
Fig. 14: Correlation strength $b_{\rm corr}$ at $\sqrt{s} = 7$ TeV for separated η-φ windows in different $p_{\rm T}$ intervals with same $\langle n_{\rm ch}\rangle$. Five $\varphi_{\rm sep}$ values are shown as a function of $\eta_{\rm sep}$. Windows of $\delta\eta$=0.2 and $\delta\varphi$=π/4. Top and bottom panels and contain the same experimental data, lines correspond to PYTHIA6 Perugia 2011 (top) and to PHOJET (bottom).

$\eta_{\rm gap} = 0$ (Fig. 12). One sees that the imposed condition $\langle n_{\rm F}\rangle$=*const* eliminates the dependence of $b_{\rm corr}$ on the multiplicity. The ratio $1/\sigma_{n_{\rm F}}^2$ decreases and $b_{\rm corr}^{\rm mod}$ increases with increasing $p_{\rm T}^{\rm min}$.

As mentioned above, in the approach used in [16] the dependence of the correlation strength on the $p_{\rm T}^{\rm min}$ of charged particles was studied without cuts on $p_{\rm T}^{\rm max}$, which leads to a decrease of the correlation $b_{\rm corr}$ with increasing $p_{\rm T}^{\rm min}$. This result can also be illustrated with the help of Eq. 7. In this case $\langle n_{\rm F}\rangle$ decreases with increasing $p_{\rm T}^{\rm min}$ and $\langle n_{\rm F}\rangle/\sigma_{n_{\rm F}}^2$ increases (approaching the Poisson limit $\sigma_{n_{\rm F}}^2 = \langle n_{\rm F}\rangle$) leading to the decrease of $b_{\rm corr}^{\rm mod}$. Thus, the difference of the results in these two approaches can be qualitatively understood using Eq. 7.

Fig. 13 shows $b_{\rm corr}$ as function of $\eta_{\rm gap}$ for different $p_{\rm T}$ intervals. Fig. 13 (a) compares data to PYTHIA6 tune Perugia 2011. The general trend of $b_{\rm corr}$ increasing with higher $p_{\rm T}^{\rm min}$ for all $\eta_{\rm gap}$ is reproduced by this tune, with small quantitative deviations. Fig. 13 (b) shows the same data in comparison to PHOJET. This generator does not describe the data well: PHOJET results are almost independent of $p_{\rm T}^{\rm min}$ and only grow significantly for the $p_{\rm T}$ range 1.03–6.00 (GeV/c). Since experimental data was used to determine the $p_{\rm T}$ intervals with the same mean multiplicity, the values of mean multiplicities may vary slightly in case of the MC samples for the same $p_{\rm T}$ intervals. Deviations from the mean value are within 4% for PYTHIA6 Perugia 0 and 12% for PHOJET.

The analysis of $b_{\rm corr}$ is also performed in η-φ separated windows in different $p_{\rm T}$ intervals with the same mean multiplicity (for pp collisions at $\sqrt{s} = 7$ TeV) in 8×8 η-φ windows. Results are shown in Fig. 14 and compared to PYTHIA6 and PHOJET calculations. In addition to the conclusions that were drawn above from the correlations between η-separated windows, some new details are revealed. In particular, one observes that the PHOJET discrepancy with the data is especially dramatic at $\varphi_{\rm sep}$=π/2, where PHOJET shows no dependence of $b_{\rm corr}$ on the $p_{\rm T}$ range. It was shown already in [47] that PHOJET has difficulties in description of underlying event measurements.

Fig. 14 shows that for higher $p_{\rm T}$ intervals a near-side peak appears (see panels for $\varphi_{\rm sep} = 0$ and π/4),

13

at the same time the b_{corr} in the flat region at $\eta_{sep} > 1$ increases with p_{T} for all φ_{sep} values (compare panels for $\varphi_{\mathrm{sep}} = \pi/2$, $3\pi/4$ and π). It should be emphasized that the value of the pedestal (the common constant component in all panels) increases with p_{T}.

In near- and away-side azimuthal regions the increase of b_{corr} with $p_{\mathrm{T}}^{\mathrm{min}}$ can be explained by an enhanced number of back-to-back decays and jets. The general rise of b_{corr} can be related to the increase of the variance σ_N^2 in Eq. 6, discussed in the framework of the simple model in Section 3.2.

6   Conclusion

The strengths of forward-backward (FB) multiplicity correlations have been measured in minimum bias pp collisions at $\sqrt{s} = 0.9$, 2.76 and 7 TeV using multiplicities determined in two separated pseudorapidity windows separated by a variable gap, η_{gap}, of up to 1.2 units. The dependences of the correlation coefficient b_{corr} on the collision energy, the width and the position of pseudorapidity windows have been investigated. For the first time, the analysis has been also applied for various configurations of the azimuthal sectors selected within these pseudorapidity windows in events at $\sqrt{s} = 0.9$ and 7 TeV.

A considerable increase of the FB correlation strength with the growth of the collision energy from $\sqrt{s} = 0.9$ to 7 TeV is observed. It is shown that this cannot be explained by the increase of the mean multiplicity alone. The correlation strength grows with the width of pseudorapidity windows, while it decreases slightly with increasing pseudorapidity gap between the windows. It is shown that there is a strong non-linear dependence of the correlation strength on the width of the pseudorapidity windows and hence on the mean multiplicity value.

Measurements of the correlation strength for various configurations of azimuthal sectors enable the distinction of two contributions: short-range (SR) and long-range (LR) correlations. A weak dependence on the collision energy is observed for the SR component while the LR component has a strong dependence. For η-gaps larger than one unit of pseudorapidity and $\pi/2$ in azimuth the LR contribution dominates. This contribution forms a pedestal value (the common constant component) of b_{corr} increasing with collision energy.

Moreover, pseudorapidity and pseudorapidity-azimuthal distributions of b_{corr} have been obtained in pp events at $\sqrt{s} = 7$ TeV for various particle transverse momentum intervals. It is found that the FB correlation strength increases with the transverse momentum if p_{T}-intervals with the same mean multiplicity are chosen.

The measurements have been compared to calculations using the PYTHIA and PHOJET MC event generators. These generators are able to describe the general trends of b_{corr} as a function of $\delta\eta$, η_{gap} and φ_{sep} and its dependence on the collision energy. In p_{T}-dependent analysis of b_{corr}, PYTHIA describes data reasonably well, while PHOJET fails to describe b_{corr} in azimuthal sectors. The observed dependences of b_{corr} add new constraints on phenomenological models. In particular the transition between soft and hard processes in pp collisions can be investigated in detail using the p_{T} dependence of azimuthal and pseudorapidity distributions of forward-backward multiplicity correlation strength b_{corr}.

References

[1] G. Alner *et al.*, "Ua5: A general study of proton-antiproton physics at $\sqrt{s} = 546$ gev," *Phys. Rep.* **154** (1987) 247.

[2] A. Capella, U. Sukhatme, C.-I. Tan, and J. T. T. Van, "Dual parton model," *Phys. Rep.* **236** (1994) 225.

[3] **UA5 Collaboration**, R. Ansorge *et al.*, "Charged Particle Correlations in $\bar{P}P$ Collisions at c.m. Energies of 200-GeV, 546-GeV and 900-GeV," *Z.Phys.* **C37** (1988) 191.

[4] S. Uhlig, I. Derado, R. Meinke, and H. Preissner, "Observation of Charged Particle Correlations Between the Forward and Backward Hemispheres in pp Collisions at ISR Energies," *Nucl.Phys.* **B132** (1978) 15.

[5] A. Capella and J. Tran Thanh Van, "Long Range Rapidity Correlations in Hadron - Nucleus Interactions," *Phys.Rev.* **D29** (1984) 2512.

[6] G. Fowler, E. Friedlander, F. Pottag, R. Weiner, J. Wheeler, *et al.*, "Rapidity Scaling of Multiplicity Distributions in a Quantum Statistical Approach," *Phys.Rev.* **D37** (1988) 3127.

[7] A. Capella and A. Krzywicki, "Unitarity Corrections to short range order: Long range rapidity correlations," *Phys.Rev.* **D18** (1978) 4120.

[8] **TASSO Collaboration**, W. Braunschweig *et al.*, "Charged Multiplicity Distributions and Correlations in e+ e- Annihilation at PETRA Energies," *Z.Phys.* **C45** (1989) 193.

[9] **DELPHI Collaboration**, P. Abreu *et al.*, "Charged particle multiplicity distributions in Z0 hadronic decays," *Z.Phys.* **C50** (1991) 185.

[10] **OPAL Collaboration**, R. Akers *et al.*, "Multiplicity and transverse momentum correlations in multihadronic final states in e+ e- interactions at $\sqrt{s} = 91.2$ GeV," *Phys.Lett.* **B320** (1994) 417.

[11] C. Bromberg, D. Chaney, D. H. Cohen, T. Ferbel, P. Slattery, *et al.*, "Pion Production in p p Collisions at 102-GeV/c.," *Phys.Rev.* **D9** (1974) 1864.

[12] **E735 Collaboration**, T. Alexopoulos *et al.*, "Charged particle multiplicity correlations in $p\bar{p}$ collisions at $\sqrt{s} = 0.3$-TeV to 1.8-TeV," *Phys.Lett.* **B353** (1995) 155.

[13] **British-French-Scandinavian Collaboration**, M. Albrow *et al.*, "Studies of Proton Proton Collisions at the CERN ISR With an Identified Charged Hadron of High Transverse Momentum at 90-degrees. 2. On the Distribution of Charged Particles in the Central Region," *Nucl.Phys.* **B145** (1978) 305.

[14] M. Derrick, K. Gan, P. Kooijman, J. Loos, B. Musgrave, *et al.*, "Study of Quark Fragmentation in e+ e- Annihilation at 29-GeV: Charged Particle Multiplicity and Single Particle Rapidity Distributions," *Phys.Rev.* **D34** (1986) 3304.

[15] **UA5 Collaboration**, K. Alpgard *et al.*, "Forward-Backward Multiplicity Correlations in p anti-p Collisions at 540-GeV," *Phys.Lett.* **B123** (1983) 361.

[16] **ATLAS Collaboration**, G. Aad *et al.*, "Forward-backward correlations and charged-particle azimuthal distributions in pp interactions using the ATLAS detector," *JHEP* **07** (2012) 019, `arXiv:1203.3100 [hep-ex]`.

[17] **STAR Collaboration**, B. Abelev *et al.*, "Growth of Long Range Forward-Backward Multiplicity Correlations with Centrality in Au+Au Collisions at $\sqrt{s_{NN}} = 200$ GeV," *Phys.Rev.Lett.* **103** (2009) 172301, `arXiv:0905.0237 [nucl-ex]`.

[18] V. Abramovsky, E. Gedalin, E. Gurvich, and O. Kancheli, "Long Range Azimuthal Correlations in Multiple Production Processes at High-energies," *JETP Lett.* **47** (1988) 337.

[19] M. Braun, C. Pajares, and V. Vechernin, "On the forward - backward correlations in a two stage scenario," *Phys.Lett.* **B493** (2000) 54, `arXiv:hep-ph/0007241 [hep-ph]`.

[20] P. Brogueira, J. Dias de Deus, and J. G. Milhano, "Forward-Backward rapidity correlations at all rapidities," *Phys.Rev.* **C76** (2007) 064901, `arXiv:0709.3913 [hep-ph]`.

[21] A. Kaidalov, "The Quark-Gluon Structure of the Pomeron and the Rise of Inclusive Spectra at High-Energies," *Phys.Lett.* **B116** (1982) 459.

[22] A. Kaidalov and K. Ter-Martirosian, "Pomeron as Quark-Gluon Strings and Multiple Hadron Production at SPS Collider Energies," *Phys.Lett.* **B117** (1982) 247.

[23] N. Amelin, N. Armesto, M. Braun, E. Ferreiro, and C. Pajares, "Long and short range correlations and the search of the quark gluon plasma," *Phys.Rev.Lett.* **73** (1994) 2813.

[24] M. Braun and C. Pajares, "Implications of percolation of color strings on multiplicities, correlations and the transverse momentum," *Eur.Phys.J.* **C16** (2000) 349, arXiv:hep-ph/9907332 [hep-ph].

[25] M. Braun, R. Kolevatov, C. Pajares, and V. Vechernin, "Correlations between multiplicities and average transverse momentum in the percolating color strings approach," *Eur.Phys.J.* **C32** (2004) 535, arXiv:hep-ph/0307056 [hep-ph].

[26] V. Vechernin and R. Kolevatov, "On multiplicity and transverse-momentum correlations in collisions of ultrarelativistic ions," *Phys.Atom.Nucl.* **70** (2007) 1797.

[27] M. Braun and C. Pajares, "Particle production in nuclear collisions and string interactions," *Phys.Lett.* **B287** (1992) 154.

[28] M. Braun and C. Pajares, "A probabilistic model of interacting strings," *Nucl.Phys.* **B390** (1993) 542.

[29] N. Armesto, M. Braun, E. Ferreiro, and C. Pajares, "Strangeness enhancement and string fusion in nucleus-nucleus collisions," *Phys.Lett.* **B344** (1995) 301.

[30] N. Amelin, N. Armesto, C. Pajares, and D. Sousa, "Monte Carlo model for nuclear collisions from SPS to LHC energies," *Eur.Phys.J.* **C22** (2001) 149, arXiv:hep-ph/0103060 [hep-ph].

[31] L. McLerran, "What is the Color Glass Condensate?," *Nucl.Phys.* **A699** (2002) 73.

[32] N. Armesto, L. McLerran, and C. Pajares, "Long Range Forward-Backward Correlations and the Color Glass Condensate," *Nucl.Phys.* **A781** (2007) 201, arXiv:hep-ph/0607345 [hep-ph].

[33] A. Dumitru, F. Gelis, L. McLerran, and R. Venugopalan, "Glasma flux tubes and the near side ridge phenomenon at RHIC," *Nucl.Phys.* **A810** (2008) 91, arXiv:0804.3858 [hep-ph].

[34] Y. V. Kovchegov, E. Levin, and L. D. McLerran, "Large scale rapidity correlations in heavy ion collisions," *Phys.Rev.* **C63** (2001) 024903, arXiv:hep-ph/9912367 [hep-ph].

[35] **ALICE Collaboration**, K. Aamodt *et al.*, "The ALICE experiment at the CERN LHC," *JINST* **3** (2008) S08002.

[36] T. Sjostrand, S. Mrenna, and P. Z. Skands, "PYTHIA 6.4 Physics and Manual," *JHEP* **05** (2006) 026, arXiv:hep-ph/0603175 [hep-ph].

[37] R. Engel, "Photoproduction within the two component dual parton model. 1. Amplitudes and cross-sections," *Z.Phys.* **C66** (1995) 203.

[38] R. Engel and J. Ranft, "Hadronic photon-photon interactions at high-energies," *Phys.Rev.* **D54** (1996) 4244, arXiv:hep-ph/9509373 [hep-ph].

[39] R. Brun, F. Bruyant, M. Maire, A. McPherson, and P. Zanarini, "GEANT3," Tech. Rep. CERN-DD-EE-84-1, CERN, 1987.

[40] V. Vechernin, "Long-Range Rapidity Correlations in the Model with Independent Emitters," in *Relativistic Nuclear Physics and Quantum Chromodynamics: Proc. of the XX Intern. Baldin Seminar on High Energy Physics Problems*, vol. 2, p. 10. JINR, Dubna, 2011. `arXiv:1012.0214 [hep-ph]`.

[41] V. Vechernin, "Forward-backward correlations between multiplicities in windows separated in azimuth and rapidity," *Nucl.Phys.* **A939** (2015) 21, `arXiv:1210.7588 [hep-ph]`.

[42] V. Vechernin, "On description of the correlation between multiplicities in windows separated in azimuth and rapidity," *PoS* **QFTHEP2013** (2013) 055, `arXiv:1305.0857 [hep-ph]`.

[43] C. Pruneau, S. Gavin, and S. Voloshin, "Methods for the study of particle production fluctuations," *Phys.Rev.* **C66** (2002) 044904, `arXiv:nucl-ex/0204011 [nucl-ex]`.

[44] A. Buckley, J. Butterworth, S. Gieseke, D. Grellscheid, S. Hoche, *et al.*, "General-purpose event generators for LHC physics," *Phys.Rept.* **504** (2011) 145, `arXiv:1101.2599 [hep-ph]`.

[45] P. Z. Skands, "Tuning Monte Carlo Generators: The Perugia Tunes," *Phys.Rev.* **D82** (2010) 074018, `arXiv:1005.3457 [hep-ph]`.

[46] K. Wraight and P. Skands, "Forward-Backward Correlations and Event Shapes as probes of Minimum-Bias Event Properties," *Eur.Phys.J.* **C71** (2011) 1628, `arXiv:1101.5215 [hep-ph]`.

[47] **ALICE Collaboration**, B. Abelev *et al.*, "Underlying Event measurements in *pp* collisions at $\sqrt{s} = 0.9$ and 7 TeV with the ALICE experiment at the LHC," *JHEP* **07** (2012) 116, `arXiv:1112.2082 [hep-ex]`.

A A model with random uniform distribution of produced particles in pseudorapidity

In a simple model with event-by-event multiplicity fluctuations and random uniform distribution of produced particles in pseudorapidity the probability to observe $n_{\rm F}$ particles in some subinterval $\delta\eta$ from the total number of N charged particles produced in the whole pseudorapidity interval Y is given by the binomial distribution:

$$P_N(n_{\rm F}) = C_N^{n_{\rm F}} p^{n_{\rm F}} (1-p)^{N-n_{\rm F}} , \tag{A.1}$$

with $\langle n_{\rm F}\rangle_N = pN$ and $\langle n_F^2\rangle_N = p(1-p)N + p^2 N^2$, where $p \equiv \delta\eta/Y$. (We consider the case of symmetric windows $\delta\eta_{\rm F} = \delta\eta_B = \delta\eta$.) Averaging then over events with different values of N,

$$P(n_{\rm F}) = \sum_N P(N) P_N(n_{\rm F}) , \tag{A.2}$$

we have

$$\langle n_{\rm F}\rangle = \sum_{n_{\rm F}} P(n_{\rm F}) n_{\rm F} = \sum_{n_{\rm F}} \sum_N P(N) P_N(n_{\rm F}) n_{\rm F} = \sum_N P(N) pN = p \langle N\rangle \tag{A.3}$$

and hence

$$p = \frac{\langle n_{\rm F}\rangle}{\langle N\rangle} = \frac{\langle n_{\rm B}\rangle}{\langle N\rangle} = \frac{\delta\eta}{Y} . \tag{A.4}$$

In the same way we find

$$\langle n_{\rm F}^2\rangle = \langle n_{\rm B}^2\rangle = p(1-p)\langle N\rangle + p^2\langle N^2\rangle , \tag{A.5}$$

$$\langle (n_{\rm F} + n_{\rm B})^2\rangle = 2p(1-2p)\langle N\rangle + (2p)^2\langle N^2\rangle . \tag{A.6}$$

One can rewrite (A.4)–(A.6) also as

$$\frac{\sigma_{n_{\rm F}+n_{\rm B}}^2 - \langle n_{\rm F} + n_{\rm B}\rangle}{\langle n_{\rm F} + n_{\rm B}\rangle^2} = \frac{\sigma_{n_{\rm F}}^2 - \langle n_{\rm F}\rangle}{\langle n_{\rm F}\rangle^2} = \frac{\sigma_{\rm N}^2 - \langle N\rangle}{\langle N\rangle^2} \equiv R_{\rm N} , \tag{A.7}$$

since the so-called robust variance R_N is the same for any subinterval of Y in the case of the independent homogeneous distribution of the particles along Y [43].

Using the presentation for the covariance

$$\langle n_F n_B \rangle - \langle n_F \rangle \langle n_B \rangle \equiv \frac{1}{2}(\sigma^2_{n_F+n_B} - \sigma^2_{n_F} - \sigma^2_{n_B}) \; , \tag{A.8}$$

we can write for the correlation coefficient in a model-independent way:

$$b_{corr} = \frac{\sigma^2_{n_F+n_B} - \sigma^2_{n_F} - \sigma^2_{n_B}}{2\sigma^2_{n_F}} \; . \tag{A.9}$$

Then combining (A.7) and (A.9) we find

$$b^{mod}_{corr} = \frac{\langle n_F \rangle R_N}{1 + \langle n_F \rangle R_N} \; . \tag{A.10}$$

Using (A.4) we can write (A.10) also as

$$b^{mod}_{corr} = \frac{\alpha \delta \eta / Y}{1 + \alpha \delta \eta / Y} \; , \tag{A.11}$$

where

$$\alpha = \langle N \rangle R_N = \frac{\sigma^2_N}{\langle N \rangle} - 1 \; . \tag{A.12}$$

Substituting the expression

$$R_N = \frac{\sigma^2_{n_F} - \langle n_F \rangle}{\langle n_F \rangle^2} \tag{A.13}$$

from (A.7) into (A.10) one finds another presentation for b^{mod}_{corr}:

$$b^{mod}_{corr} = 1 - \frac{\langle n_F \rangle}{\sigma^2_{n_F}} \; . \tag{A.14}$$

B   The ALICE Collaboration

J. Adam[40], D. Adamová[83], M.M. Aggarwal[87], G. Aglieri Rinella[36], M. Agnello[111], N. Agrawal[48],
Z. Ahammed[131], I. Ahmed[16], S.U. Ahn[68], I. Aimo[94,111], S. Aiola[136], M. Ajaz[16], A. Akindinov[58],
S.N. Alam[131], D. Aleksandrov[100], B. Alessandro[111], D. Alexandre[102], R. Alfaro Molina[64], A. Alici[105,12],
A. Alkin[3], J. Alme[38], T. Alt[43], S. Altinpinar[18], I. Altsybeev[130], C. Alves Garcia Prado[119], C. Andrei[78],
A. Andronic[97], V. Anguelov[93], J. Anielski[54], T. Antičić[98], F. Antinori[108], P. Antonioli[105], L. Aphecetche[113],
H. Appelshäuser[53], S. Arcelli[28], N. Armesto[17], R. Arnaldi[111], T. Aronsson[136], I.C. Arsene[22], M. Arslandok[53],
A. Augustinus[36], R. Averbeck[97], M.D. Azmi[19], M. Bach[43], A. Badalà[107], Y.W. Baek[44], S. Bagnasco[111],
R. Bailhache[53], R. Bala[90], A. Baldisseri[15], M. Ball[92], F. Baltasar Dos Santos Pedrosa[36], R.C. Baral[61],
A.M. Barbano[111], R. Barbera[29], F. Barile[33], G.G. Barnaföldi[135], L.S. Barnby[102], V. Barret[70], P. Bartalini[7],
J. Bartke[116], E. Bartsch[53], M. Basile[28], N. Bastid[70], S. Basu[131], B. Bathen[54], G. Batigne[113], A. Batista
Camejo[70], B. Batyunya[66], P.C. Batzing[22], I.G. Bearden[80], H. Beck[53], C. Bedda[111], N.K. Behera[48],
I. Belikov[55], F. Bellini[28], H. Bello Martinez[2], R. Bellwied[121], R. Belmont[134], E. Belmont-Moreno[64],
V. Belyaev[76], G. Bencedi[135], S. Beole[27], I. Berceanu[78], A. Bercuci[78], Y. Berdnikov[85], D. Berenyi[135],
R.A. Bertens[57], D. Berzano[36], L. Betev[36], A. Bhasin[90], I.R. Bhat[90], A.K. Bhati[87], B. Bhattacharjee[45],
J. Bhom[127], L. Bianchi[27,121], N. Bianchi[72], C. Bianchin[57], J. Bielčík[40], J. Bielčíková[83], A. Bilandzic[80],
S. Biswas[79], S. Bjelogrlic[57], F. Blanco[10], D. Blau[100], C. Blume[53], F. Bock[74,93], A. Bogdanov[76],
H. Bøggild[80], L. Boldizsár[135], M. Bombara[41], J. Book[53], H. Borel[15], A. Borissov[96], M. Borri[82], F. Bossú[65],
M. Botje[81], E. Botta[27], S. Böttger[52], P. Braun-Munzinger[97], M. Bregant[119], T. Breitner[52], T.A. Broker[53],
T.A. Browning[95], M. Broz[40], E.J. Brucken[46], E. Bruna[111], G.E. Bruno[33], D. Budnikov[99], H. Buesching[53],
S. Bufalino[36,111], P. Buncic[36], O. Busch[93], Z. Buthelezi[65], J.T. Buxton[20], D. Caffarri[30,36], X. Cai[7],
H. Caines[136], L. Calero Diaz[72], A. Caliva[57], E. Calvo Villar[103], P. Camerini[26], F. Carena[36], W. Carena[36],
J. Castillo Castellanos[15], A.J. Castro[124], E.A.R. Casula[25], C. Cavicchioli[36], C. Ceballos Sanchez[9], J. Cepila[40],
P. Cerello[111], B. Chang[122], S. Chapeland[36], M. Chartier[123], J.L. Charvet[15], S. Chattopadhyay[131],
S. Chattopadhyay[101], V. Chelnokov[3], M. Cherney[86], C. Cheshkov[129], B. Cheynis[129], V. Chibante Barroso[36],
D.D. Chinellato[120], P. Chochula[36], K. Choi[96], M. Chojnacki[80], S. Choudhury[131], P. Christakoglou[81],
C.H. Christensen[80], P. Christiansen[34], T. Chujo[127], S.U. Chung[96], C. Cicalo[106], L. Cifarelli[12,28],
F. Cindolo[105], J. Cleymans[89], F. Colamaria[33], D. Colella[33], A. Collu[25], M. Colocci[28], G. Conesa Balbastre[71],
Z. Conesa del Valle[51], M.E. Connors[136], J.G. Contreras[11,40], T.M. Cormier[84], Y. Corrales Morales[27], I. Cortés
Maldonado[2], P. Cortese[32], M.R. Cosentino[119], F. Costa[36], P. Crochet[70], R. Cruz Albino[11], E. Cuautle[63],
L. Cunqueiro[36], T. Dahms[92,37], A. Dainese[108], A. Danu[62], D. Das[101], I. Das[51,101], S. Das[4], A. Dash[120],
S. Dash[48], S. De[131,119], A. De Caro[31,12], G. de Cataldo[104], J. de Cuveland[43], A. De Falco[25], D. De
Gruttola[12,31], N. De Marco[111], S. De Pasquale[31], A. Deloff[77], E. Dénes[135], G. D'Erasmo[33], D. Di Bari[33],
A. Di Mauro[36], P. Di Nezza[72], M.A. Diaz Corchero[10], T. Dietel[89], P. Dillenseger[53], R. Divià[36],
Ø. Djuvsland[18], A. Dobrin[57,81], T. Dobrowolski[77,i], D. Domenicis Gimenez[119], B. Dönigus[53], O. Dordic[22],
A.K. Dubey[131], A. Dubla[57], L. Ducroux[129], P. Dupieux[70], R.J. Ehlers[136], D. Elia[104], H. Engel[52],
B. Erazmus[113,36], H.A. Erdal[38], D. Eschweiler[43], B. Espagnon[51], M. Esposito[36], M. Estienne[113], S. Esumi[127],
D. Evans[102], S. Evdokimov[112], G. Eyyubova[40], L. Fabbietti[37,92], D. Fabris[108], J. Faivre[71], A. Fantoni[72],
M. Fasel[74], L. Feldkamp[54], D. Felea[62], A. Feliciello[111], G. Feofilov[130], J. Ferencei[83], A. Fernández Téllez[2],
E.G. Ferreiro[17], A. Ferretti[27], A. Festanti[30], J. Figiel[116], M.A.S. Figueredo[123], S. Filchagin[99], D. Finogeev[56],
F.M. Fionda[104], E.M. Fiore[33], M.G. Fleck[93], M. Floris[36], S. Foertsch[65], P. Foka[97], S. Fokin[100],
E. Fragiacomo[110], A. Francescon[36,30], U. Frankenfeld[97], U. Fuchs[36], C. Furget[71], A. Furs[56], M. Fusco
Girard[31], J.J. Gaardhøje[80], M. Gagliardi[27], A.M. Gago[103], M. Gallio[27], D.R. Gangadharan[74], P. Ganoti[88],
C. Gao[7], C. Garabatos[97], E. Garcia-Solis[13], C. Gargiulo[36], P. Gasik[37,92], M. Germain[113], A. Gheata[36],
M. Gheata[62,36], B. Ghidini[33], P. Ghosh[131], S.K. Ghosh[4], P. Gianotti[72], P. Giubellino[36], P. Giubilato[30],
E. Gladysz-Dziadus[116], P. Glässel[93], A. Gomez Ramirez[52], P. González-Zamora[10], S. Gorbunov[43],
L. Görlich[116], S. Gotovac[115], V. Grabski[64], L.K. Graczykowski[133], A. Grelli[57], A. Grigoras[36], C. Grigoras[36],
V. Grigoriev[76], A. Grigoryan[1], S. Grigoryan[66], B. Grinyov[3], N. Grion[110], J.F. Grosse-Oetringhaus[36],
J.-Y. Grossiord[129], R. Grosso[36], F. Guber[56], R. Guernane[71], B. Guerzoni[28], K. Gulbrandsen[80], H. Gulkanyan[1],
T. Gunji[126], A. Gupta[90], R. Gupta[90], R. Haake[54], Ø. Haaland[18], C. Hadjidakis[51], M. Haiduc[62],
H. Hamagaki[126], G. Hamar[135], L.D. Hanratty[102], A. Hansen[80], J.W. Harris[136], H. Hartmann[43], A. Harton[13],
D. Hatzifotiadou[105], S. Hayashi[126], S.T. Heckel[53], M. Heide[54], H. Helstrup[38], A. Herghelegiu[78], G. Herrera
Corral[11], B.A. Hess[35], K.F. Hetland[38], T.E. Hilden[46], H. Hillemanns[36], B. Hippolyte[55], P. Hristov[36],
M. Huang[18], T.J. Humanic[20], N. Hussain[45], T. Hussain[19], D. Hutter[43], D.S. Hwang[21], R. Ilkaev[99], I. Ilkiv[77],
M. Inaba[127], C. Ionita[36], M. Ippolitov[76,100], M. Irfan[19], M. Ivanov[97], V. Ivanov[85], A. Jachołkowski[29],
P.M. Jacobs[74], C. Jahnke[119], H.J. Jang[68], M.A. Janik[133], P.H.S.Y. Jayarathna[121], C. Jena[30], S. Jena[121],

R.T. Jimenez Bustamante[63], P.G. Jones[102], H. Jung[44], A. Jusko[102], P. Kalinak[59], A. Kalweit[36], J. Kamin[53], J.H. Kang[137], V. Kaplin[76], S. Kar[131], A. Karasu Uysal[69], O. Karavichev[56], T. Karavicheva[56], E. Karpechev[56], U. Kebschull[52], R. Keidel[138], D.L.D. Keijdener[57], M. Keil[36], K.H. Khan[16], M.M. Khan[19], P. Khan[101], S.A. Khan[131], A. Khanzadeev[85], Y. Kharlov[112], B. Kileng[38], B. Kim[137], D.W. Kim[68 ,44], D.J. Kim[122], H. Kim[137], J.S. Kim[44], M. Kim[44], M. Kim[137], S. Kim[21], T. Kim[137], S. Kirsch[43], I. Kisel[43], S. Kiselev[58], A. Kisiel[133], G. Kiss[135], J.L. Klay[6], C. Klein[53], J. Klein[93], C. Klein-Bösing[54], A. Kluge[36], M.L. Knichel[93], A.G. Knospe[117], T. Kobayashi[127], C. Kobdaj[114], M. Kofarago[36], M.K. Köhler[97], T. Kollegger[43 ,97], A. Kolojvari[130], V. Kondratiev[130], N. Kondratyeva[76], E. Kondratyuk[112], A. Konevskikh[56], V. Kovalenko[130], M. Kowalski[36 ,116], S. Kox[71], G. Koyithatta Meethaleveedu[48], J. Kral[122], I. Králik[59], A. Kravčáková[41], M. Krelina[40], M. Kretz[43], M. Krivda[59 ,102], F. Krizek[83], E. Kryshen[36], M. Krzewicki[43 ,97], A.M. Kubera[20], V. Kučera[83], Y. Kucheriaev[100 ,i], T. Kugathasan[36], C. Kuhn[55], P.G. Kuijer[81], I. Kulakov[43], J. Kumar[48], L. Kumar[87 ,79], P. Kurashvili[77], A. Kurepin[56], A.B. Kurepin[56], A. Kuryakin[99], S. Kushpil[83], M.J. Kweon[50], Y. Kwon[137], S.L. La Pointe[111], P. La Rocca[29], C. Lagana Fernandes[119], I. Lakomov[51 ,36], R. Langoy[42], C. Lara[52], A. Lardeux[15], A. Lattuca[27], E. Laudi[36], R. Lea[26], L. Leardini[93], G.R. Lee[102], I. Legrand[36], J. Lehnert[53], R.C. Lemmon[82], V. Lenti[104], E. Leogrande[57], I. León Monzón[118], M. Leoncino[27], P. Lévai[135], S. Li[7 ,70], X. Li[14], J. Lien[42], R. Lietava[102], S. Lindal[22], V. Lindenstruth[43], C. Lippmann[97], M.A. Lisa[20], H.M. Ljunggren[34], D.F. Lodato[57], P.I. Loenne[18], V.R. Loggins[134], V. Loginov[76], C. Loizides[74], X. Lopez[70], E. López Torres[9], A. Lowe[135], X.-G. Lu[93], P. Luettig[53], M. Lunardon[30], G. Luparello[26 ,57], A. Maevskaya[56], M. Mager[36], S. Mahajan[90], S.M. Mahmood[22], A. Maire[55], R.D. Majka[136], M. Malaev[85], I. Maldonado Cervantes[63], L. Malinina[66], D. Mal'Kevich[58], P. Malzacher[97], A. Mamonov[99], L. Manceau[111], V. Manko[100], F. Manso[70], V. Manzari[104 ,36], M. Marchisone[27], J. Mareš[60], G.V. Margagliotti[26], A. Margotti[105], J. Margutti[57], A. Marín[97], C. Markert[117], M. Marquard[53], I. Martashvili[124], N.A. Martin[97], J. Martin Blanco[113], P. Martinengo[36], M.I. Martínez[2], G. Martínez García[113], Y. Martynov[3], A. Mas[119], S. Masciocchi[97], M. Masera[27], A. Masoni[106], L. Massacrier[113], A. Mastroserio[33], A. Matyja[116], C. Mayer[116], J. Mazer[124], M.A. Mazzoni[109], D. Mcdonald[121], F. Meddi[24], A. Menchaca-Rocha[64], E. Meninno[31], J. Mercado Pérez[93], M. Meres[39], Y. Miake[127], M.M. Mieskolainen[46], K. Mikhaylov[58 ,66], L. Milano[36], J. Milosevic[22 ,132], L.M. Minervini[104 ,23], A. Mischke[57], A.N. Mishra[49], D. Miśkowiec[97], J. Mitra[131], C.M. Mitu[62], N. Mohammadi[57], B. Mohanty[131 ,79], L. Molnar[55], L. Montaño Zetina[11], E. Montes[10], M. Morando[30], D.A. Moreira De Godoy[113], S. Moretto[30], A. Morreale[113], A. Morsch[36], V. Muccifora[72], E. Mudnic[115], D. Mühlheim[54], S. Muhuri[131], M. Mukherjee[131], H. Müller[36], J.D. Mulligan[136], M.G. Munhoz[119], S. Murray[65], L. Musa[36], J. Musinsky[59], B.K. Nandi[48], R. Nania[105], E. Nappi[104], M.U. Naru[16], C. Nattrass[124], K. Nayak[79], T.K. Nayak[131], S. Nazarenko[99], A. Nedosekin[58], L. Nellen[63], F. Ng[121], M. Nicassio[97], M. Niculescu[36 ,62], J. Niedziela[36], B.S. Nielsen[80], S. Nikolaev[100], S. Nikulin[100], V. Nikulin[85], B.S. Nilsen[86], F. Noferini[105 ,12], P. Nomokonov[66], G. Nooren[57], J. Norman[123], A. Nyanin[100], J. Nystrand[18], H. Oeschler[93], S. Oh[136], S.K. Oh[67], A. Ohlson[36], A. Okatan[69], T. Okubo[47], L. Olah[135], J. Oleniacz[133], A.C. Oliveira Da Silva[119], J. Onderwaater[97], C. Oppedisano[111], A. Ortiz Velasquez[63 ,34], A. Oskarsson[34], J. Otwinowski[97 ,116], K. Oyama[93], M. Ozdemir[53], Y. Pachmayer[93], P. Pagano[31], G. Paić[63], C. Pajares[17], S.K. Pal[131], J. Pan[134], A.K. Pandey[48], D. Pant[48], V. Papikyan[1], G.S. Pappalardo[107], P. Pareek[49], W.J. Park[97], S. Parmar[87], A. Passfeld[54], D.I. Patalakha[112], V. Paticchio[104], B. Paul[101], T. Pawlak[133], T. Peitzmann[57], H. Pereira Da Costa[15], E. Pereira De Oliveira Filho[119], D. Peresunko[76 ,100], C.E. Pérez Lara[81], V. Peskov[53], Y. Pestov[5], V. Petráček[40], V. Petrov[112], M. Petrovici[78], C. Petta[29], S. Piano[110], M. Pikna[39], P. Pillot[113], O. Pinazza[105 ,36], L. Pinsky[121], D.B. Piyarathna[121], M. Płoskoń[74], M. Planinic[128], J. Pluta[133], S. Pochybova[135], P.L.M. Podesta-Lerma[118], M.G. Poghosyan[86], B. Polichtchouk[112], N. Poljak[128], W. Poonsawat[114], A. Pop[78], S. Porteboeuf-Houssais[70], J. Porter[74], J. Pospisil[83], S.K. Prasad[4], R. Preghenella[36 ,105 ,12], F. Prino[111], C.A. Pruneau[134], I. Pshenichnov[56], M. Puccio[111], G. Puddu[25], P. Pujahari[134], V. Punin[99], J. Putschke[134], H. Qvigstad[22], A. Rachevski[110], S. Raha[4], S. Rajput[90], J. Rak[122], A. Rakotozafindrabe[15], L. Ramello[32], R. Raniwala[91], S. Raniwala[91], S.S. Räsänen[46], B.T. Rascanu[53], D. Rathee[87], A.W. Rauf[16], V. Razazi[25], K.F. Read[124], J.S. Real[71], K. Redlich[77], R.J. Reed[136 ,134], A. Rehman[18], P. Reichelt[53], M. Reicher[57], F. Reidt[93 ,36], R. Renfordt[53], A.R. Reolon[72], A. Reshetin[56], F. Rettig[43], J.-P. Revol[12], K. Reygers[93], V. Riabov[85], R.A. Ricci[73], T. Richert[34], M. Richter[22], P. Riedler[36], W. Riegler[36], F. Riggi[29], C. Ristea[62], A. Rivetti[111], E. Rocco[57], M. Rodríguez Cahuantzi[11 ,2], A. Rodriguez Manso[81], K. Røed[22], E. Rogochaya[66], D. Rohr[43], D. Röhrich[18], R. Romita[123], F. Ronchetti[72], L. Ronflette[113], P. Rosnet[70], A. Rossi[36], F. Roukoutakis[88], A. Roy[49], C. Roy[55], P. Roy[101], A.J. Rubio Montero[10], R. Rui[26], R. Russo[27], E. Ryabinkin[100], Y. Ryabov[85], A. Rybicki[116], S. Sadovsky[112], K. Šafařík[36], B. Sahlmuller[53], P. Sahoo[49], R. Sahoo[49], S. Sahoo[61], P.K. Sahu[61], J. Saini[131], S. Sakai[72], M.A. Saleh[134], C.A. Salgado[17], J. Salzwedel[20], S. Sambyal[90], V. Samsonov[85], X. Sanchez Castro[55], L. Šándor[59], A. Sandoval[64], M. Sano[127], G. Santagati[29],

D. Sarkar[131], E. Scapparone[105], F. Scarlassara[30], R.P. Scharenberg[95], C. Schiaua[78], R. Schicker[93], C. Schmidt[97], H.R. Schmidt[35], S. Schuchmann[53], J. Schukraft[36], M. Schulc[40], T. Schuster[136], Y. Schutz[113,36], K. Schwarz[97], K. Schweda[97], G. Scioli[28], E. Scomparin[111], R. Scott[124], K.S. Seeder[119], G. Segato[30], J.E. Seger[86], Y. Sekiguchi[126], I. Selyuzhenkov[97], K. Senosi[65], J. Seo[67,96], E. Serradilla[64,10], A. Sevcenco[62], A. Shabanov[56], A. Shabetai[113], O. Shadura[3], R. Shahoyan[36], A. Shangaraev[112], A. Sharma[90], N. Sharma[61,124], K. Shigaki[47], K. Shtejer[27,9], Y. Sibiriak[100], S. Siddhanta[106], K.M. Sielewicz[36], T. Siemiarczuk[77], D. Silvermyr[84,34], C. Silvestre[71], G. Simatovic[128], R. Singaraju[131], R. Singh[90,79], S. Singha[79,131], V. Singhal[131], B.C. Sinha[131], T. Sinha[101], B. Sitar[39], M. Sitta[32], T.B. Skaali[22], K. Skjerdal[18], M. Slupecki[122], N. Smirnov[136], R.J.M. Snellings[57], T.W. Snellman[122], C. Søgaard[34], R. Soltz[75], J. Song[96], M. Song[137], Z. Song[7], F. Soramel[30], S. Sorensen[124], M. Spacek[40], E. Spiriti[72], I. Sputowska[116], M. Spyropoulou-Stassinaki[88], B.K. Srivastava[95], J. Stachel[93], I. Stan[62], G. Stefanek[77], M. Steinpreis[20], E. Stenlund[34], G. Steyn[65], J.H. Stiller[93], D. Stocco[113], P. Strmen[39], A.A.P. Suaide[119], T. Sugitate[47], C. Suire[51], M. Suleymanov[16], R. Sultanov[58], M. Šumbera[83], T.J.M. Symons[74], A. Szabo[39], A. Szanto de Toledo[119,i], I. Szarka[39], A. Szczepankiewicz[36], M. Szymanski[133], J. Takahashi[120], N. Tanaka[127], M.A. Tangaro[33], J.D. Tapia Takaki[ii,51], A. Tarantola Peloni[53], M. Tariq[19], M.G. Tarzila[78], A. Tauro[36], G. Tejeda Muñoz[2], A. Telesca[36], K. Terasaki[126], C. Terrevoli[30,25], B. Teyssier[129], J. Thäder[97,74], D. Thomas[57,117], R. Tieulent[129], A.R. Timmins[121], A. Toia[53], S. Trogolo[111], V. Trubnikov[3], W.H. Trzaska[122], T. Tsuji[126], A. Tumkin[99], R. Turrisi[108], T.S. Tveter[22], K. Ullaland[18], A. Uras[129], G.L. Usai[25], A. Utrobicic[128], M. Vajzer[83], M. Vala[59], L. Valencia Palomo[70], S. Vallero[27], J. Van Der Maarel[57], J.W. Van Hoorne[36], M. van Leeuwen[57], T. Vanat[83], P. Vande Vyvre[36], D. Varga[135], A. Vargas[2], M. Vargyas[122], R. Varma[48], M. Vasileiou[88], A. Vasiliev[100], A. Vauthier[71], V. Vechernin[130], A.M. Veen[57], M. Veldhoen[57], A. Velure[18], M. Venaruzzo[73], E. Vercellin[27], S. Vergara Limón[2], R. Vernet[8], M. Verweij[134], L. Vickovic[115], G. Viesti[30,i], J. Viinikainen[122], Z. Vilakazi[125,65], O. Villalobos Baillie[102], A. Vinogradov[100], L. Vinogradov[130], Y. Vinogradov[99], T. Virgili[31], V. Vislavicius[34], Y.P. Viyogi[131], A. Vodopyanov[66], M.A. Völkl[93], K. Voloshin[58], S.A. Voloshin[134], G. Volpe[36], B. von Haller[36], I. Vorobyev[92,37], D. Vranic[97,36], J. Vrláková[41], B. Vulpescu[70], A. Vyushin[99], B. Wagner[18], J. Wagner[97], H. Wang[57], M. Wang[7,113], Y. Wang[93], D. Watanabe[127], M. Weber[36,121], S.G. Weber[97], J.P. Wessels[54], U. Westerhoff[54], J. Wiechula[35], J. Wikne[22], M. Wilde[54], G. Wilk[77], J. Wilkinson[93], M.C.S. Williams[105], B. Windelband[93], M. Winn[93], C.G. Yaldo[134], Y. Yamaguchi[126], H. Yang[57], P. Yang[7], S. Yano[47], S. Yasnopolskiy[100], Z. Yin[7], H. Yokoyama[127], I.-K. Yoo[96], V. Yurchenko[3], I. Yushmanov[100], A. Zaborowska[133], V. Zaccolo[80], A. Zaman[16], C. Zampolli[105], H.J.C. Zanoli[119], S. Zaporozhets[66], A. Zarochentsev[130], P. Závada[60], N. Zaviyalov[99], H. Zbroszczyk[133], I.S. Zgura[62], M. Zhalov[85], H. Zhang[7], X. Zhang[74], Y. Zhang[7], C. Zhao[22], N. Zhigareva[58], D. Zhou[7], Y. Zhou[57], Z. Zhou[18], H. Zhu[7], J. Zhu[7,113], X. Zhu[7], A. Zichichi[12,28], A. Zimmermann[93], M.B. Zimmermann[54,36], G. Zinovjev[3], M. Zyzak[43]

Affiliation notes

[i] Deceased
[ii] Also at: University of Kansas, Lawrence, Kansas, United States

Collaboration Institutes

[1] A.I. Alikhanyan National Science Laboratory (Yerevan Physics Institute) Foundation, Yerevan, Armenia
[2] Benemérita Universidad Autónoma de Puebla, Puebla, Mexico
[3] Bogolyubov Institute for Theoretical Physics, Kiev, Ukraine
[4] Bose Institute, Department of Physics and Centre for Astroparticle Physics and Space Science (CAPSS), Kolkata, India
[5] Budker Institute for Nuclear Physics, Novosibirsk, Russia
[6] California Polytechnic State University, San Luis Obispo, California, United States
[7] Central China Normal University, Wuhan, China
[8] Centre de Calcul de l'IN2P3, Villeurbanne, France
[9] Centro de Aplicaciones Tecnológicas y Desarrollo Nuclear (CEADEN), Havana, Cuba
[10] Centro de Investigaciones Energéticas Medioambientales y Tecnológicas (CIEMAT), Madrid, Spain
[11] Centro de Investigación y de Estudios Avanzados (CINVESTAV), Mexico City and Mérida, Mexico
[12] Centro Fermi - Museo Storico della Fisica e Centro Studi e Ricerche "Enrico Fermi", Rome, Italy
[13] Chicago State University, Chicago, Illinois, USA
[14] China Institute of Atomic Energy, Beijing, China

[15] Commissariat à l'Energie Atomique, IRFU, Saclay, France

[16] COMSATS Institute of Information Technology (CIIT), Islamabad, Pakistan

[17] Departamento de Física de Partículas and IGFAE, Universidad de Santiago de Compostela, Santiago de Compostela, Spain

[18] Department of Physics and Technology, University of Bergen, Bergen, Norway

[19] Department of Physics, Aligarh Muslim University, Aligarh, India

[20] Department of Physics, Ohio State University, Columbus, Ohio, United States

[21] Department of Physics, Sejong University, Seoul, South Korea

[22] Department of Physics, University of Oslo, Oslo, Norway

[23] Dipartimento di Elettrotecnica ed Elettronica del Politecnico, Bari, Italy

[24] Dipartimento di Fisica dell'Università 'La Sapienza' and Sezione INFN Rome, Italy

[25] Dipartimento di Fisica dell'Università and Sezione INFN, Cagliari, Italy

[26] Dipartimento di Fisica dell'Università and Sezione INFN, Trieste, Italy

[27] Dipartimento di Fisica dell'Università and Sezione INFN, Turin, Italy

[28] Dipartimento di Fisica e Astronomia dell'Università and Sezione INFN, Bologna, Italy

[29] Dipartimento di Fisica e Astronomia dell'Università and Sezione INFN, Catania, Italy

[30] Dipartimento di Fisica e Astronomia dell'Università and Sezione INFN, Padova, Italy

[31] Dipartimento di Fisica 'E.R. Caianiello' dell'Università and Gruppo Collegato INFN, Salerno, Italy

[32] Dipartimento di Scienze e Innovazione Tecnologica dell'Università del Piemonte Orientale and Gruppo Collegato INFN, Alessandria, Italy

[33] Dipartimento Interateneo di Fisica 'M. Merlin' and Sezione INFN, Bari, Italy

[34] Division of Experimental High Energy Physics, University of Lund, Lund, Sweden

[35] Eberhard Karls Universität Tübingen, Tübingen, Germany

[36] European Organization for Nuclear Research (CERN), Geneva, Switzerland

[37] Excellence Cluster Universe, Technische Universität München, Munich, Germany

[38] Faculty of Engineering, Bergen University College, Bergen, Norway

[39] Faculty of Mathematics, Physics and Informatics, Comenius University, Bratislava, Slovakia

[40] Faculty of Nuclear Sciences and Physical Engineering, Czech Technical University in Prague, Prague, Czech Republic

[41] Faculty of Science, P.J. Šafárik University, Košice, Slovakia

[42] Faculty of Technology, Buskerud and Vestfold University College, Vestfold, Norway

[43] Frankfurt Institute for Advanced Studies, Johann Wolfgang Goethe-Universität Frankfurt, Frankfurt, Germany

[44] Gangneung-Wonju National University, Gangneung, South Korea

[45] Gauhati University, Department of Physics, Guwahati, India

[46] Helsinki Institute of Physics (HIP), Helsinki, Finland

[47] Hiroshima University, Hiroshima, Japan

[48] Indian Institute of Technology Bombay (IIT), Mumbai, India

[49] Indian Institute of Technology Indore, Indore (IITI), India

[50] Inha University, Incheon, South Korea

[51] Institut de Physique Nucléaire d'Orsay (IPNO), Université Paris-Sud, CNRS-IN2P3, Orsay, France

[52] Institut für Informatik, Johann Wolfgang Goethe-Universität Frankfurt, Frankfurt, Germany

[53] Institut für Kernphysik, Johann Wolfgang Goethe-Universität Frankfurt, Frankfurt, Germany

[54] Institut für Kernphysik, Westfälische Wilhelms-Universität Münster, Münster, Germany

[55] Institut Pluridisciplinaire Hubert Curien (IPHC), Université de Strasbourg, CNRS-IN2P3, Strasbourg, France

[56] Institute for Nuclear Research, Academy of Sciences, Moscow, Russia

[57] Institute for Subatomic Physics of Utrecht University, Utrecht, Netherlands

[58] Institute for Theoretical and Experimental Physics, Moscow, Russia

[59] Institute of Experimental Physics, Slovak Academy of Sciences, Košice, Slovakia

[60] Institute of Physics, Academy of Sciences of the Czech Republic, Prague, Czech Republic

[61] Institute of Physics, Bhubaneswar, India

[62] Institute of Space Science (ISS), Bucharest, Romania

[63] Instituto de Ciencias Nucleares, Universidad Nacional Autónoma de México, Mexico City, Mexico

[64] Instituto de Física, Universidad Nacional Autónoma de México, Mexico City, Mexico

[65] iThemba LABS, National Research Foundation, Somerset West, South Africa

[66] Joint Institute for Nuclear Research (JINR), Dubna, Russia
[67] Konkuk University, Seoul, South Korea
[68] Korea Institute of Science and Technology Information, Daejeon, South Korea
[69] KTO Karatay University, Konya, Turkey
[70] Laboratoire de Physique Corpusculaire (LPC), Clermont Université, Université Blaise Pascal, CNRS–IN2P3, Clermont-Ferrand, France
[71] Laboratoire de Physique Subatomique et de Cosmologie, Université Grenoble-Alpes, CNRS-IN2P3, Grenoble, France
[72] Laboratori Nazionali di Frascati, INFN, Frascati, Italy
[73] Laboratori Nazionali di Legnaro, INFN, Legnaro, Italy
[74] Lawrence Berkeley National Laboratory, Berkeley, California, United States
[75] Lawrence Livermore National Laboratory, Livermore, California, United States
[76] Moscow Engineering Physics Institute, Moscow, Russia
[77] National Centre for Nuclear Studies, Warsaw, Poland
[78] National Institute for Physics and Nuclear Engineering, Bucharest, Romania
[79] National Institute of Science Education and Research, Bhubaneswar, India
[80] Niels Bohr Institute, University of Copenhagen, Copenhagen, Denmark
[81] Nikhef, National Institute for Subatomic Physics, Amsterdam, Netherlands
[82] Nuclear Physics Group, STFC Daresbury Laboratory, Daresbury, United Kingdom
[83] Nuclear Physics Institute, Academy of Sciences of the Czech Republic, Řež u Prahy, Czech Republic
[84] Oak Ridge National Laboratory, Oak Ridge, Tennessee, United States
[85] Petersburg Nuclear Physics Institute, Gatchina, Russia
[86] Physics Department, Creighton University, Omaha, Nebraska, United States
[87] Physics Department, Panjab University, Chandigarh, India
[88] Physics Department, University of Athens, Athens, Greece
[89] Physics Department, University of Cape Town, Cape Town, South Africa
[90] Physics Department, University of Jammu, Jammu, India
[91] Physics Department, University of Rajasthan, Jaipur, India
[92] Physik Department, Technische Universität München, Munich, Germany
[93] Physikalisches Institut, Ruprecht-Karls-Universität Heidelberg, Heidelberg, Germany
[94] Politecnico di Torino, Turin, Italy
[95] Purdue University, West Lafayette, Indiana, United States
[96] Pusan National University, Pusan, South Korea
[97] Research Division and ExtreMe Matter Institute EMMI, GSI Helmholtzzentrum für Schwerionenforschung, Darmstadt, Germany
[98] Rudjer Bošković Institute, Zagreb, Croatia
[99] Russian Federal Nuclear Center (VNIIEF), Sarov, Russia
[100] Russian Research Centre Kurchatov Institute, Moscow, Russia
[101] Saha Institute of Nuclear Physics, Kolkata, India
[102] School of Physics and Astronomy, University of Birmingham, Birmingham, United Kingdom
[103] Sección Física, Departamento de Ciencias, Pontificia Universidad Católica del Perú, Lima, Peru
[104] Sezione INFN, Bari, Italy
[105] Sezione INFN, Bologna, Italy
[106] Sezione INFN, Cagliari, Italy
[107] Sezione INFN, Catania, Italy
[108] Sezione INFN, Padova, Italy
[109] Sezione INFN, Rome, Italy
[110] Sezione INFN, Trieste, Italy
[111] Sezione INFN, Turin, Italy
[112] SSC IHEP of NRC Kurchatov institute, Protvino, Russia
[113] SUBATECH, Ecole des Mines de Nantes, Université de Nantes, CNRS-IN2P3, Nantes, France
[114] Suranaree University of Technology, Nakhon Ratchasima, Thailand
[115] Technical University of Split FESB, Split, Croatia
[116] The Henryk Niewodniczanski Institute of Nuclear Physics, Polish Academy of Sciences, Cracow, Poland
[117] The University of Texas at Austin, Physics Department, Austin, Texas, USA
[118] Universidad Autónoma de Sinaloa, Culiacán, Mexico

[119] Universidade de São Paulo (USP), São Paulo, Brazil
[120] Universidade Estadual de Campinas (UNICAMP), Campinas, Brazil
[121] University of Houston, Houston, Texas, United States
[122] University of Jyväskylä, Jyväskylä, Finland
[123] University of Liverpool, Liverpool, United Kingdom
[124] University of Tennessee, Knoxville, Tennessee, United States
[125] University of the Witwatersrand, Johannesburg, South Africa
[126] University of Tokyo, Tokyo, Japan
[127] University of Tsukuba, Tsukuba, Japan
[128] University of Zagreb, Zagreb, Croatia
[129] Université de Lyon, Université Lyon 1, CNRS/IN2P3, IPN-Lyon, Villeurbanne, France
[130] V. Fock Institute for Physics, St. Petersburg State University, St. Petersburg, Russia
[131] Variable Energy Cyclotron Centre, Kolkata, India
[132] Vinča Institute of Nuclear Sciences, Belgrade, Serbia
[133] Warsaw University of Technology, Warsaw, Poland
[134] Wayne State University, Detroit, Michigan, United States
[135] Wigner Research Centre for Physics, Hungarian Academy of Sciences, Budapest, Hungary
[136] Yale University, New Haven, Connecticut, United States
[137] Yonsei University, Seoul, South Korea
[138] Zentrum für Technologietransfer und Telekommunikation (ZTT), Fachhochschule Worms, Worms, Germany